Mathematics

AIMS Mathematics, 11(5): 13865–13912.
DOI: 10.3934/math.2026571
Received: 03 March 2026
Revised: 22 April 2026
Accepted: 24 April 2026
Published: 18 May 2026

https://www.aimspress.com/journal/Math

Research article

A unified parsimonious exponential-G family for modeling real-world data: theory and statistical inference

Eman M. Eldemery[1], Hisham M. Almongy[2], Khaled M. Mahfouz[1], Mohammed M. El Genidy[1], Ibrahim Elbatal[2,*], Hassan M. Aljohani[3] and Ahmed Z. Afify[4]

[1] Department of Mathematics and Computer Science, Faculty of Science, Port Said University, Port Said, Egypt
[2] Department of Mathematics and Statistics, College of Science, Imam Mohammad Ibn Saud Islamic University (IMSIU), Riyadh 11432, Saudi Arabia
[3] Department of Mathematics and Statistics, College of Science, Taif University, P. O. Box 11099, Taif 21944, Saudi Arabia
[4] Department of Statistics, Mathematics, and Insurance, Benha University, Benha 13511, Egypt

* **Correspondence:** Email: iielbatal@imamu.edu.sa.

Abstract: This paper introduces a new parsimonious class of statistical models, called the flexible exponential-G (FEx-G) family. The primary motivation for proposing the FEx-G family lies in its structural simplicity and adaptability, as it accommodates any baseline distribution without introducing additional shape parameters, thereby avoiding unnecessary model complexity. Unlike many existing generator-based families, the FEx-G family is independent of previously established generators, making it a distinct and original contribution to distribution theory. Despite its parsimonious structure, the FEx-G family exhibits remarkable flexibility, being capable of modeling both monotone and nonmonotone failure rate functions, and therefore is suitable for analyzing a wide range of non-negative real-world data. A special case, termed the flexible exponential-Kumaraswamy (FExKw) distribution, is investigated in detail. The parameters of the FExKw model are estimated using nine different estimation methods, and extensive simulation studies are conducted to evaluate and rank their performance. The practical usefulness of the FExKw distribution is illustrated through applications to four real-life datasets from environmental science, industry, and medicine, where it demonstrates superior performance compared with several well-established competing distributions.

Keywords: Kumaraswamy distribution; T–X family; simulations; real data; maximum likelihood; mean residual life; failure rate

Mathematics Subject Classification: 60E05, 62F10, 62N05

1. Introduction

Recently, statisticians have expressed an increasing interest in developing generator-based families or generalized models by adding parameters to existing baseline distributions. These improved models offer greater flexibility, allowing for more accurate modeling of real-life data across various applied fields, including economics, biology, engineering, industry, computer science, medicine, insurance, and life testing. The classical distributions exhibit limitations in flexibility and possess relatively restricted qualities in practical data, making flexibly generated models critical for better fits and deeper insights in such applications.

Several well-known generator families are the Kumaraswamy-G [1], transmuted exponentiated generalized-G [2], Weibull-G [3], Marshall–Olkin-G [4], transmuted-G [5], Kumaraswamy transmuted-G [6], generalized odd log-logistic-G [7], Marshall–Olkin–Weibull-G [8], beta-G [9], modified generalized-G [10], generalized transmuted-G [11], flexible Lomax-G [12], flexible exponential-G [13], and modified Kavya–Manoharan-G [14] families.

Kavya and Manoharan [15] presented a novel transformation called the Kavya–Manoharan-G (KM-G) class. This transformation resulted in the creation of several extended versions of classical distributions with the goal of increasing the model's flexibility and adaptability. Notable examples include the KM Burr X [16], KM inverse length-biased exponential [17], KM log-logistic [18], KM Kumaraswamy [19], KM Kumaraswamy exponential [20], and KM power-Lomax distributions [21]. These extended models improve the ability to accurately fit and analyze diverse datasets across a variety of statistical domains.

The primary objective of this article is to introduce the flexible exponential-G (FEx-G) family as a new transformation-based extension within the general transformed-transformer (T–X) framework. The proposed family is designed to have desirable statistical properties while also effectively modeling a wide range of real-world data across multiple application areas. The chief motivation behind the proposed FEx-G family is its ability to accommodate a wide range of failure rate shapes without adding any additional parameters to the baseline models. Furthermore, the proposed FEx-G family of distributions is not derived from any existing parent family such as the Marshall–Olkin-G (MO-G) [4], exponentiated-G (E-G) (Lehmann Types I and II) [22], transmuted-G (T-G) [5], cubic rank transmuted-G [23], and exponentiated-generalized-G (EG-G) [24] families. This independence from previously established generators represents a distinctive feature and was a key motivation for developing the FEx-G family.

Furthermore, compared with other generated families within the T–X framework, the proposed FEx-G family introduces a distinct transformation mechanism through the term $\bar{G}(x)^{G(x)}$, which differs from commonly used generators such as the exponential, beta, or Kumaraswamy transformations. Unlike existing models, the proposed construction leads to a more flexible hazard rate function (HRF), including the ability to capture nonmonotonic shapes such as bathtub and unimodal forms, while maintaining a parsimonious structure without introducing additional shape parameters. Moreover, the resulting linear representation in terms of exponentiated-G densities provides additional analytical tractability that is not typically available in closely related families.

The main contribution of the proposed FEx-G family lies in introducing extra distributional

flexibility through a nonstandard interaction between the baseline cumulative distribution function (CDF) and the survival function (SF), while preserving the dimensionality of the baseline model. This feature distinguishes it from many existing families, such as the Kumaraswamy, Marshall–Olkin, and beta families, which typically achieve flexibility by incorporating additional shape parameters. In contrast, the proposed FEx-G family achieves enhanced flexibility through the transformation $W[G(x)] = 1 - \bar{G}(x)^{G(x)}$ without enlarging the parameter space. As a result, it provides a parsimonious alternative in settings where interpretability, estimation stability, and avoidance of overparameterization are important. The practical relevance of this feature is further demonstrated in the real data applications, where the proposed model shows strong competitiveness and, in several cases, superior performance compared with the baseline and competing models.

In practical terms, this setting may be especially useful when the baseline distribution is not flexible enough to capture the observed pattern of the data, particularly in the presence of more complex density or hazard rate behavior, while a more highly parameterized extension may be less desirable. Thus, the proposed family provides a useful compromise between flexibility and structural simplicity. The practical value of this feature is illustrated in Section 8 through four real data applications from environmental, industrial, and medical settings, where the proposed model demonstrates highly competitive performance and, in several cases, provides a better fit than the baseline and other competing distributions according to the adopted goodness-of-fit criteria.

The motivation for developing this family stems from a desire to better the efficiency and flexibility of traditional distribution methods. The FEx-G family's submodels can accommodate a variety of HRF shapes, including increasing, J-shaped, decreasing, reversed-J, upside-down bathtub, bathtub, and modified bathtub. The probability density functions in these models can be right-skewed, unimodal, symmetric, reversed-J, left-skewed, J-shaped, or bimodal. To demonstrate the FEx-G family’s versatility, five baseline distributions—Kumaraswamy, Weibull, exponential, gamma, and beta—are used to generate five distinct submodels: The FEx-Kumaraswamy (FExKw), FEx-Weilbull (FExW), FEx-exponential (FExEx), FEx-gamma (FExGa), and FEx-beta (FExB) distributions.

Recent work on distribution theory continues to emphasize the development of flexible probability models with useful mathematical properties and strong empirical performance. For instance, Bouhadjar et al. [25] introduced the Bouhadjar distribution and examined its mathematical properties, simulation behavior, and applications. Saaidia et al. [26] proposed the Q-Lindley distribution for lifetime and reliability data and assessed its performance through goodness-of-fit tests, simulation, and real data analysis. In a similar direction, the Xbeta distribution [27] was introduced as a flexible model, and its properties, estimation procedures, and practical applications were also investigated. These contributions reflect the continuing interest in constructing parsimonious yet adaptable distributions for modeling complex real-world data.

Specifically, nine approaches are used to estimate the FExKw model's parameters. The effectiveness of these estimation techniques is assessed through extensive simulation studies, noting that moment-based estimation has recently shown high accuracy in related settings such as generalized extreme value modeling [28,29]. Finally, the practical utility of the proposed models is demonstrated by applying them to four real-world datasets from environmental, industrial, and medical fields, demonstrating the FEx-G family's flexibility and effectiveness.

The advantages of the proposed FEx-G transformation relative to the baseline distribution should be stated more clearly. First, unlike many generated families that increase flexibility by

introducing additional shape parameters, the FEx-G family preserves the dimensionality of the baseline model while still allowing for richer distributional behavior. In particular, under suitable parameter settings, the proposed transformation can generate more flexible hazard rate patterns, including nonmonotone shapes that may not be adequately captured by the baseline model alone. Second, as illustrated analytically in Section 5.2 and supported empirically in Section 8, the proposed FEx-G submodels can provide a highly competitive fit to real-world data without increasing the model's complexity. Third, this parsimonious structure may be especially attractive in applications where the baseline model is too restrictive to describe the observed data pattern, whereas a more heavily parameterized extension may be less desirable because of interpretability or estimation concerns. Taken together, these points help clarify the practical and comparative motivation for the proposed approach.

The rest of the paper is organized as follows: The FEx-G family of distributions is introduced in Section 2. Section 3 presents five specific submodels within this family. Section 4 discusses the key properties of the FEx-G family. In Section 5, important properties of the FExKw distribution are obtained. Estimation methods for the FExKw distribution parameters are detailed in Section 6. Simulation results are reported in Section 7, while Section 8 presents four real-life applications. Finally, Section 9 concludes the paper with some closing remarks.

2. Formation of the FEx-G family

In this section, we define the proposed FEx-G family based on the T–X approach introduced by Alzaatreh et al. [30]. Let $r(t)$ and $R(t)$ denote the probability density function (PDF) and CDF of a random variable (RV) T supported on (a, b), where $-\infty < a < b < \infty$. Let $G(x)$ be the baseline CDF and $\bar{G}(x) = 1 - G(x)$ its SF.

The CDF of the T–X family is defined by

$$F_{TX}(x) = \int_a^{W[G(x)]} r(t)\, dt = R\{W[G(x)]\}. \tag{2.1}$$

The corresponding PDF of (2.1) reduces to

$$f_{TX}(x) = r\{W[G(x)]\}\frac{d}{dx}W[G(x)].$$

The T–X construction requires that $W[G(x)]$ satisfies the following three conditions:

(i) $W[G(x)] \in (a, b)$.

(ii) $W[G(x)]$ is differentiable and monotonically nondecreasing.

(iii) $\lim_{x\to-\infty} W[G(x)] = a$ and $\lim_{x\to+\infty} W[G(x)] = b$.

To construct the proposed FEx-G family, we define the transformation function explicitly as follows

$$W[G(x)] = 1 - \bar{G}(x)^{G(x)}, \text{where } \bar{G}(x) = 1 - G(x),$$

and choose

$$r(t) = p\exp(-t),\ 0 < t < 1, \text{where } p = \mathrm{e}/(\mathrm{e} - 1).$$

Since $0 < 1 - \bar{G}(x)^{G(x)} < 1$ for $G(x) \in (0,1)$, it follows that $0 < W[G(x)] < 1$, so $a = 0$

and $b = 1$.

Differentiating $W[G(x)]$, we obtain

$$\begin{aligned}\frac{d}{dx}W[G(x)] &= \frac{d}{dx}\left[1-\bar{G}(x)^{G(x)}\right] = -\frac{d}{dx}\bar{G}(x)^{G(x)} \\ &= \bar{G}(x)^{G(x)}\left[\frac{G(x)}{\bar{G}(x)}g(x) - g(x)\log\bar{G}(x)\right] \\ &= g(x)\bar{G}(x)^{G(x)}\left[\frac{G(x)}{\bar{G}(x)} - \log\bar{G}(x)\right],\end{aligned}$$

which is strictly positive for $G(x) \in (0,1)$, implying that $W[G(x)]$ is increasing. Moreover, if $G(x) \to 0$ as $x \to -\infty$ and $G(x) \to 1$ as $x \to +\infty$, then

$$\lim_{x\to-\infty} W[G(x)] = 0 \qquad \text{and} \qquad \lim_{x\to+\infty} W[G(x)] = 1.$$

Hence, the CDF of the proposed FEx-G family is

$$F(x) = \int_0^{W[G(x)]} r(t)\,dt = \int_0^{1-\bar{G}(x)^{G(x)}} p\exp(-t)\,dt = p\left(1-\exp\left\{-\left[1-\bar{G}(x)^{G(x)}\right]\right\}\right), \quad (2.2)$$

where $p = \mathrm{e}/(\mathrm{e}-1)$, $\bar{G}(x) = 1 - G(x)$, and the support of the random variable X coincides with that of the baseline distribution, i.e., $x \in \mathbb{R}$ or any subset thereof.

Indeed, since $r(t)$ is non-negative and $W[G(x)]$ is increasing in x, it follows that $F(x)$ is also nondecreasing. Moreover, if the baseline distribution satisfies $G(x) \to 0$ as $x \to -\infty$ and $G(x) \to 1$ as $x \to +\infty$, then

$$\lim_{x\to-\infty} F(x) = 0 \quad \text{and} \quad \lim_{x\to+\infty} F(x) = 1.$$

The corresponding PDF is obtained by differentiating (2.2). Using the chain rule, we have

$$f(x) = p\exp\left\{-\left[1-\bar{G}(x)^{G(x)}\right]\right\}\frac{d}{dx}\left[1-\bar{G}(x)^{G(x)}\right].$$

Substituting the derivative of $W[G(x)]$ yields

$$f(x) = p\,g(x)\,\bar{G}(x)^{G(x)}\left[\frac{G(x)}{\bar{G}(x)} - \log\bar{G}(x)\right]\exp\left\{-\left[1-\bar{G}(x)^{G(x)}\right]\right\}. \quad (2.3)$$

The HRF of the FEx-G family is described as

$$h(x) = \frac{f(x)}{1-F(x)} = \frac{p\,g(x)\,\bar{G}(x)^{G(x)}\left[\frac{G(x)}{\bar{G}(x)} - \log\bar{G}(x)\right]\exp\left\{-\left[1-\bar{G}(x)^{G(x)}\right]\right\}}{1-p\left(1-\exp\left\{-\left[1-\bar{G}(x)^{G(x)}\right]\right\}\right)}.$$

Henceforth, the RV with the PDF in (2.3) is represented as X~FEx-G($\boldsymbol{\psi}$). The FEx-G family is a genuinely parsimonious class of models: It introduces no additional parameters beyond those of the baseline distribution, yet its special submodels—demonstrated in the subsequent sections—are capable of capturing essential data features such as shape, skewness, and tail behavior without unnecessary complexity or risk of overfitting. The family remains mathematically tractable and often performs competitively or even better than more complex alternatives. Its strength lies in its ability to

accommodate a wide range of failure-rate shapes while preserving the simplicity of the original baseline models.

The proposed generator in (2.2) provides an extension of several established G classes of distributions in Table A1 (see Supplementary Data). Furthermore, the resulting flexible G-families generated from these classes are described in Table A2 (see Supplementary Data). These supplementary materials present 70 newly developed families of distributions derived from the proposed unified framework.

3. Five distinct submodels

In this section, we present five distinct submodels of the FEx-G family, namely the FExKw, FExW, FExEx, FExGa, and FExB distributions. These submodels can represent monotone and nonmonotone failure rates, including increasing, inverted J-shaped, decreasing, bathtub, modified bathtub, and upside-down bathtubs. They can have right-skewed, symmetrical, or reversed-J shaped density. Figures 1–5 illustrate all of these shapes.

3.1. The FExKw distribution

The CDF of the Kumaraswamy (Kw) distribution is given by $G(x) = 1-(1-x^a)^b$, where $x \in \mathbb{I}, a, b > 0$. The CDF of the FExKw distribution is obtained by substituting the CDF of the Kw distribution into Eq (2.2) as follows:

$$F(x) = p\left[1-\exp\left(-\left\{1-(1-x^a)^{b[1-(1-x^a)^b]}\right\}\right)\right],\ x \in \mathbb{I},\ a, b > 0. \tag{3.1}$$

The corresponding PDF of the FExKw distribution simplifies to

$$f(x) = p\,a\,b\,x^{a-1}(1-x^a)^{2b-1}(1-x^a)^{-b(1-x^a)^b}\{[(1-x^a)^{-b}-1]-b\log(1-x^a)\}\exp\left(-\left\{1-(1-x^a)^{b[1-(1-x^a)^b]}\right\}\right). \tag{3.2}$$

Figure 1 illustrates the FExKw distribution's PDF and HRF shapes.

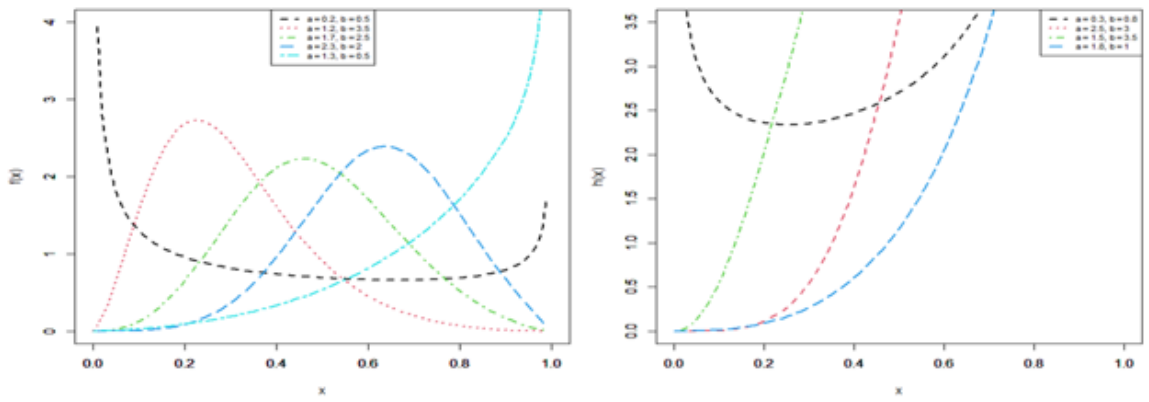


Figure 1. Plots of the PDF and HRF of the FExKw distribution.

3.2. The FExW distribution

The CDF of the Weibull (W) distribution has the form $G(x) = 1 - \exp(-\lambda\, x^{\alpha})$, where $x > 0, \lambda, \alpha > 0$. The CDF of the FExW distribution is obtained by substituting the CDF of the W distribution into Eq (2.2) as follows:

$$F(x) = p\left[1 - \exp\left(-\left\{1 - [\exp(-\lambda x^{\alpha})]^{[1-\exp(-\lambda x^{\alpha})]}\right\}\right)\right]$$

$$= p\{1 - \exp[-(1 - \exp\{-\lambda x^{\alpha}[1 - \exp(-\lambda x^{\alpha})]\})]\},\ x > 0, \lambda, \alpha > 0. \tag{3.3}$$

Figure 2 illustrates the FExW distribution's PDF and HRF shapes.

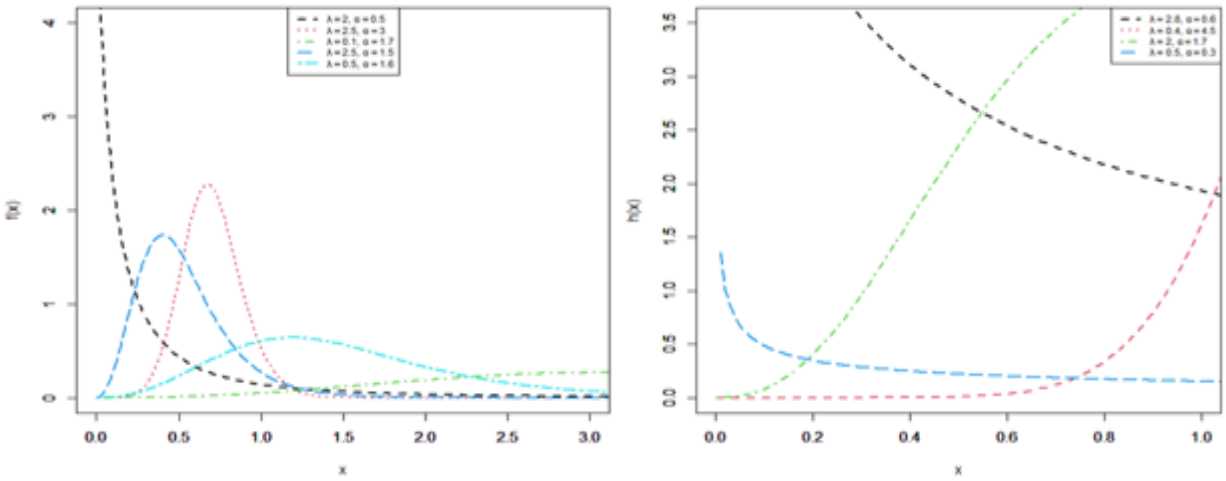


Figure 2. Plots of the PDF and HRF of the FExW distribution.

3.3. The FExEx distribution

The CDF of the exponential (Ex) distribution is defined by $G(x) = 1 - \exp(-\lambda\, x)$, where $x > 0,\ \lambda > 0$. The CDF of the FExEx distribution is as follows:

$$F(x) = p\{1 - \exp[-(1 - \exp\{-\lambda x[1 - \exp(-\lambda x)]\})]\}, x > 0,\ \lambda > 0. \tag{3.4}$$

Figure 3 illustrates the FExEx distribution's PDF and HRF shapes.

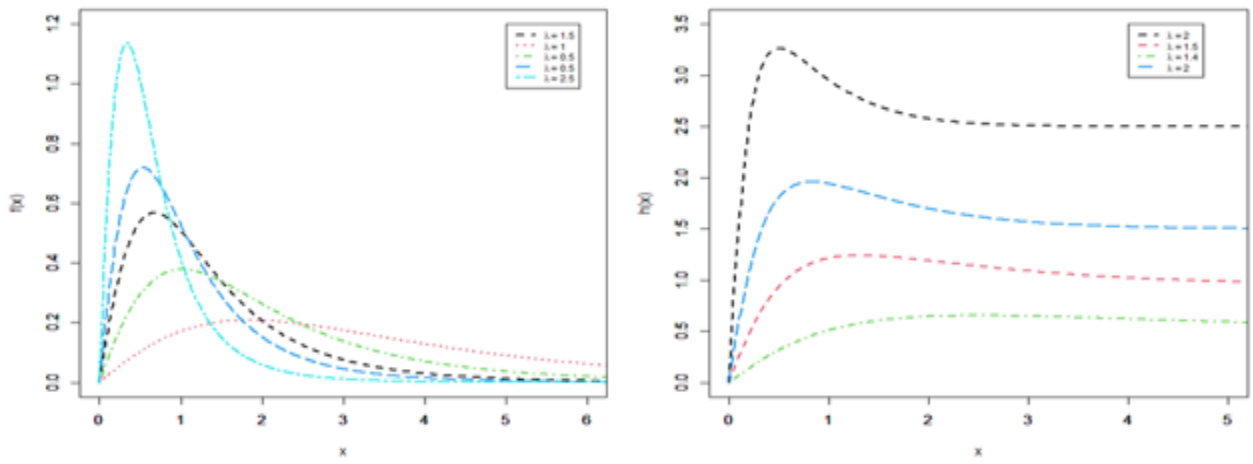


Figure 3. Plots of the PDF and HRF of the FExEx distribution.

3.4. The FExGa distribution

The CDF the gamma (Ga) distribution takes the form $G(x) = \gamma(k, x/\theta)/\Gamma(k)$, where $x > 0$, $k, \theta > 0$. The CDF of the FExGa distribution reduces to

$$F(x) = p - p\exp\left(-\left\{1 - \left[1 - \frac{\gamma(k,x/\theta)}{\Gamma(k)}\right]^{\frac{\gamma(k,x/\theta)}{\Gamma(k)}}\right\}\right), \; x > 0, \quad k, \theta > 0, \tag{3.5}$$

where $\Gamma(k) = \int_0^\infty t^{k-1}\mathrm{e}^{-t}\,dt$ and $\gamma\left(k, {}^{x}/_{\theta}\right) = \int_0^{x/\theta} t^{k-1}\mathrm{e}^{-t}\,dt$ are the Ga function and the lower incomplete Ga function, respectively.

Figure 4 illustrates the FExGa distribution's PDF and HRF shapes.

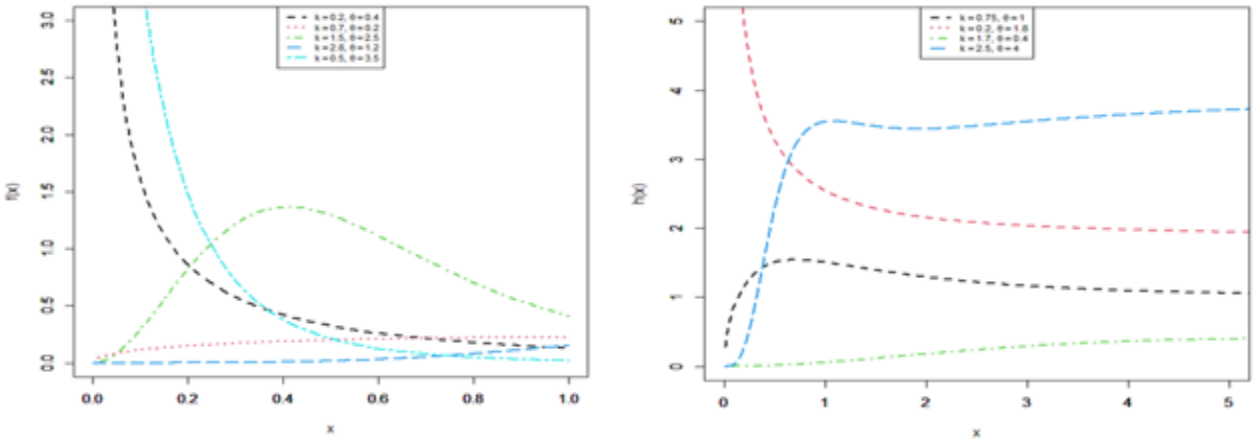


Figure 4. Plots of the PDF and HRF of the FExGa distribution.

3.5. *The FExB distribution*

The CDF of the beta (B) distribution is given by $G(x) = I_x(\alpha, \beta)$, where $x \in \mathbb{I},\ \alpha, \beta > 0$. The CDF of the FExB distribution takes the form

$$F(x) = p\left[1 - \exp\left(-\left\{1 - [1 - I_x(\alpha, \beta)]^{I_x(\alpha,\beta)}\right\}\right)\right],\ x \in \mathbb{I},\ \alpha, \beta > 0, \tag{3.6}$$

where $I_t(\alpha, \beta) = \frac{B_x(\alpha,\beta)}{B(\alpha,\beta)} = [B(\alpha, \beta)]^{-1} \int_0^x t^{\alpha-1}(1-t)^{\beta-1}\, dt$ refers to the incomplete beta function (BF) ratio, where $B(\alpha, \beta) = \int_0^1 t^{\alpha-1}(1-t)^{\beta-1}\, dt$ and $B_x(\alpha, \beta) = \int_0^x t^{\alpha-1}(1-t)^{\beta-1}\, dt$ represent the BF and incomplete BF, respectively.

Figure 5 illustrates the FExB distribution's PDF and HRF shapes.

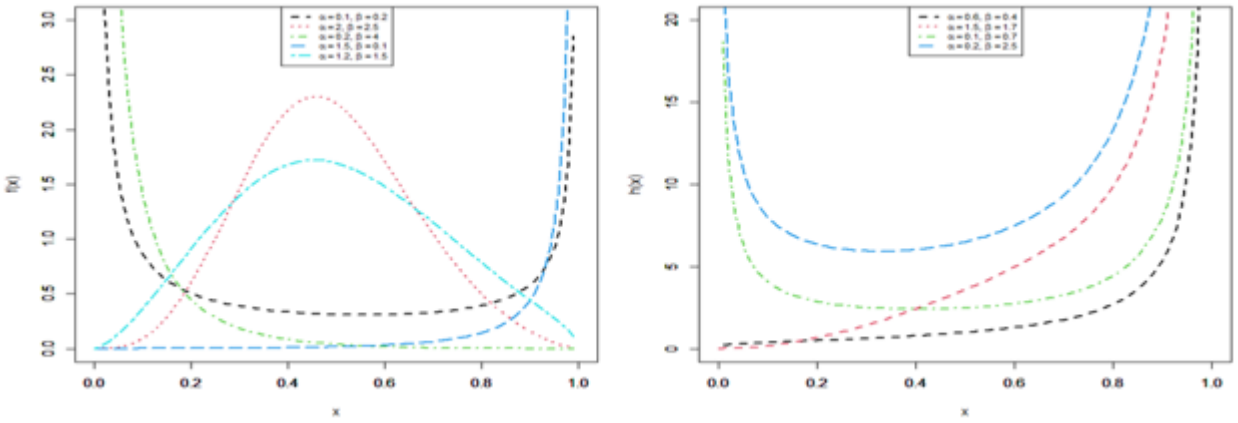


Figure 5. Plots of the PDF and HRF of the FExB distribution.

4. Properties of FEx-G family

This section explains some mathematical properties of the FEx-G family.

4.1. *Linear representation*

This section illustrates that the CDF and PDF of the FEx-G family can be expressed, based on the exponentiated-G (exp-G) density $h_k(x) = k\, g(x)G(x)^{k-1}$, with the parameter $k > 0$.

By applying the exponential series to Eq (2.2), we obtain

$$F(x) = p\left\{1 - \sum_{k=0}^{\infty} \frac{(-1)^k}{k!}\left[1 - \bar{G}(x)^{G(x)}\right]^k\right\}.$$

Since the term $\bar{G}(x)^{G(x)}$ does not have a simple polynomial form in $G(x)$, it is not straightforward to express $F(x)$ directly in powers of $G(x)$. For this reason, we use Mathematica software to obtain the following power series representation:

$$F(x) = \sum_{j=2}^{\infty} a_j\ G(x)^j, \tag{4.1}$$

where $a_2 = p, a_3 = \frac{p}{2}, a_4 = \frac{-2p}{3}$, and $a_5 = \frac{-3p}{4}$.

Equation (4.1) can be expressed as

$$F(x) = \sum_{j=2}^{\infty} a_j H_j(x), \tag{4.2}$$

where $H_j(x) = G(x)^j$ (for $j \geq 2$).

To ensure the validity of the series expansion in (4.1), we note that the exponential series expansion is valid for all finite values of its argument. Since $0 < G(x) < 1$ for all x in the support of the baseline distribution, the term $\bar{G}(x)^{G(x)}$ is well-defined and bounded. Consequently, the resulting series representation is convergent.

Furthermore, the power series representation of $F(x)$ in terms of $G(x)$ is valid for $G(x) \in (0,1)$, which holds for any proper CDF.

Moreover, the series in (4.1) is uniformly convergent on compact subsets of the support. Therefore, the term-by-term differentiation of (4.1) is justified under standard regularity conditions, permitting the interchange of differentiation and summation, yielding the corresponding expression for the PDF.

$$f(x) = \sum_{j=2}^{\infty} a_j \, j \, G(x)^{j-1} \, g(x).$$

Putting $k = j - 1$ (so $k = 1,2, \ldots$), we obtain the following index-shifted form:

$$f(x) = \sum_{k=1}^{\infty} a_{k+1} \, (k+1) \, G(x)^k \, g(x).$$

Hence, the PDF of the FEx-G family takes the form

$$f(x) = \sum_{k=1}^{\infty} a_{k+1} \, h_{k+1}(x), \tag{4.3}$$

where $h_{k+1}(x)$ is the exp-G density with a power parameter $k + 1$. Hence, Eq (4.3) illustrates that the FEx-G PDF is a linear combination of exp-G densities.

4.2. Quantile function and moments

The quantile function (QF) of X, expressed as $Q(u) = F^{-1}(u)$ for $0 < u < 1$, is obtained numerically by inverting Eq (2.2). In general, the transformation $\bar{G}(x)^{G(x)}$ does not admit a closed-form inverse, and therefore the QF of the FEx-G family is not available in an explicit closed form.

The procedure to evaluate the QF of the FEx-G family is summarized in the following three steps:

(1) Set

$$z = z(u) = 1 + \log\left(1 - \frac{u}{p}\right).$$

(2) Let

$$w = G(x) \in (0,1).$$

Since $\bar{G}(x) = 1 - G(x)$, Eq (2.2) reduces to the nonlinear equation

$$(1-w)^w = z.$$

Equivalently

$$w \log(1-w) = \log(z).$$

This equation can be solved numerically using a standard root-finding method such as the Newton–Raphson algorithm.

(3) Once w is obtained, solving $G(x) = w$ gives $x = Q(u) = G^{-1}(w)$.

Let T_{k+1} be the exp-G RV with power parameter $k+1$. The rth moment of X is derived from (4.3) as follows:

$$\mu_r{}' = E(x^r) = \sum_{k=1}^{\infty} a_{k+1}\, E(T_{k+1}^r). \tag{4.4}$$

The moment-generating function (MGF) of X, $M_X(t) = E(\mathrm{e}^{tX})$, follows from (4.3) as

$$M_X(t) = \sum_{k=1}^{\infty} a_{k+1}\, M_{k+1}(t),$$

where $M_{k+1}(t)$ represents the MGF of T_{k+1}.

Based on (4.3), the sth incomplete moment of X can be written as

$$\varphi_s(t) = \int_{-\infty}^{t} x^s\, f(x)\, dx = \sum_{k=1}^{\infty} a_{k+1} \int_{-\infty}^{t} x^s\, h_{k+1}(x)\, dx. \tag{4.5}$$

The first incomplete moment (FIM) is obtained from (4.5) when $s = 1$. It can generate Lorenz and Bonferroni curves, which are extremely useful in economics, statistics, demographics, and medicine. Now, $\varphi_1(t)$ is calculated using (4.5).

$$\varphi_1(t) = \sum_{k=1}^{\infty} a_{k+1}\, I_{k+1}(t), \tag{4.6}$$

where $I_{k+1}(t) = \int_{-\infty}^{t} x\, h_{k+1}(x)\, dx$ is the exp-G family's FIM.

The mean deviations of X around the mean $\left[\delta_1 = E\left(\left|X - \mu'_1\right|\right)\right]$ and the median $[\delta_2 = E(|X-M|)]$ are $\delta_1 = 2\,\mu'_1 F\left(\mu'_1\right) - 2\,\varphi_1\left(\mu'_1\right)$ and $\delta_2 = \mu'_1 - 2\,\varphi_1(M)$, where $\mu'_1 = E(X)$ and the median is $M = Q(0.5)$. It is simple to evaluate $F\left(\mu'_1\right)$ from (2.2).

4.3 Entropies

The Rényi entropy of a RV X is a measure of its variation in uncertainty. The Rényi entropy is described as follows:

$$R_\alpha = \frac{1}{1-\alpha} \log\left(\int_{-\infty}^{\infty} f(x)^\alpha\, dx\right), \alpha > 0 \text{ and } \alpha \neq 1.$$

Through the FEx-G density (2.3), we have

$$f(x)^\alpha = p^\alpha\, g(x)^\alpha\, \bar{G}(x)^{\alpha\, G(x)} \left[\frac{G(x)}{\bar{G}(x)} - \log \bar{G}(x)\right]^\alpha \left(\exp\left\{-\left[1 - \bar{G}(x)^{G(x)}\right]\right\}\right)^\alpha.$$

Applying the exponential series to the last term, we get

$$\left(\exp\left\{-\left[1-\bar{G}(x)^{G(x)}\right]\right\}\right)^{\alpha}=\sum_{i=0}^{\infty}\frac{(-\alpha)^{i}\left[1-\bar{G}(x)^{G(x)}\right]^{i}}{i!}.$$

Subsequently, $f(x)^{\alpha}$ reduces to

$$f(x)^{\alpha}=\sum_{i=0}^{\infty}\eta_{i}\,g(x)^{\alpha}\,\bar{G}(x)^{\alpha\,G(x)}\left[\frac{G(x)}{\bar{G}(x)}-\log\bar{G}(x)\right]^{\alpha}\left[1-\bar{G}(x)^{G(x)}\right]^{i},$$

where $\eta_{i}=\sum_{i=0}^{\infty}(-\alpha)^{i}\,p^{\alpha}/i!$.

The FEx-G family's Rényi entropy reduces to

$$R_{\alpha}=\frac{1}{1-\alpha}\left\{\log\left[\sum_{i=0}^{\infty}\eta_{i}\int_{-\infty}^{\infty}g(x)^{\alpha}\,\bar{G}(x)^{\alpha\,G(x)}\left[\frac{G(x)}{\bar{G}(x)}-\log\bar{G}(x)\right]^{\alpha}\left[1-\bar{G}(x)^{G(x)}\right]^{i}dx\right]\right\}.$$

4.4 Order statistics

Let $X_{1},\cdots,X_{n}$ represent a random sample from the FEx-G family. The PDF of $X_{i:n}$ can be expressed as

$$f_{X_{i:n}}(x)=\frac{f(x)}{B(i,n-i+1)}\sum_{j=0}^{n-i}(-1)^{j}\binom{n-i}{j}F(x)^{j+i-1},\tag{4.7}$$

where $B(.,.)$ is the BF. Through (2.2) and (2.3), we obtain

$$f(x)F(x)^{j+i-1}=p^{j+i}\,g(x)\,\bar{G}(x)^{G(x)}\left[\frac{G(x)}{\bar{G}(x)}-\log\bar{G}(x)\right]\exp\left\{-\left[1-\bar{G}(x)^{G(x)}\right]\right\}$$

$$\times\left(1-\exp\left\{-\left[1-\bar{G}(x)^{G(x)}\right]\right\}\right)^{j+i-1}.\tag{4.8}$$

Using the generalized binomial series to (4.8), we obtain

$$f(x)F(x)^{j+i-1}=p^{j+i}\sum_{s,l=0}^{\infty}\frac{(-1)^{s+l}(1+s)^{l}}{l!}\binom{j+i-1}{s}g(x)\left[1-\bar{G}(x)^{G(x)}\right]^{l}$$

$$\times\bar{G}(x)^{G(x)}\left[\frac{G(x)}{\bar{G}(x)}-\log\bar{G}(x)\right].\tag{4.9}$$

Inserting (4.9) into Eq (4.7), the PDF of $X_{i:n}$ reduces to

$$f_{X_{i:n}}(x)=\sum_{l=0}^{\infty}b_{l}\,h_{l+1}(x),\tag{4.10}$$

where $h_{l+1}(x)=(l+1)\,g(x)\,\bar{G}(x)^{G(x)}\left[\frac{G(x)}{\bar{G}(x)}-\log\bar{G}(x)\right]\left[1-\bar{G}(x)^{G(x)}\right]^{l}$ is the exp-G density with power parameter $l+1$ and

$$b_{l}=\sum_{j=0}^{n-i}\sum_{s=0}^{\infty}\frac{(-1)^{j+s+l}(1+s)^{l}}{(l+1)!}\binom{j+i-1}{s}\frac{p^{j+i}}{B(i,n-i+1)}\binom{n-i}{j}.\tag{4.11}$$

Therefore, the PDF of the FEx-G order statistics is a single linear combination of exp-G densities. Using (4.11), we can determine the properties of $X_{i:n}$ from those of T_{l+1}. For instance, the qth moment of $X_{i:n}$ is given as

$$E(X^q{}_{i:n}) = \sum_{l=0}^{\infty} b_l \, E(T^q{}_{l+1}). \tag{4.12}$$

5 Properties of the FExKw distribution

In this section, we derive some properties of the FExKw distribution.

5.1. Quantile and moments

The QF of the FExKw distribution is expressed as

$$Q(u) = \left\{1 - \left[1 + \log\left(1 - \frac{u}{p}\right)\right]^{\frac{1}{b(1-k^b)}}\right\}^{\frac{1}{a}},$$

where $k = (1 - x^a)$ and $p = \mathrm{e}/(\mathrm{e} - 1)$.

The QF can be utilized for evaluating the relationships between the parameters (a, b), as well as the skewness and kurtosis; in particular, the QF influences the Galton's skewness (GSK) and the Moors' kurtosis (MKU). Figure 6 shows the GSK and MKU for the FExKw distribution at various values of the parameters a and b.

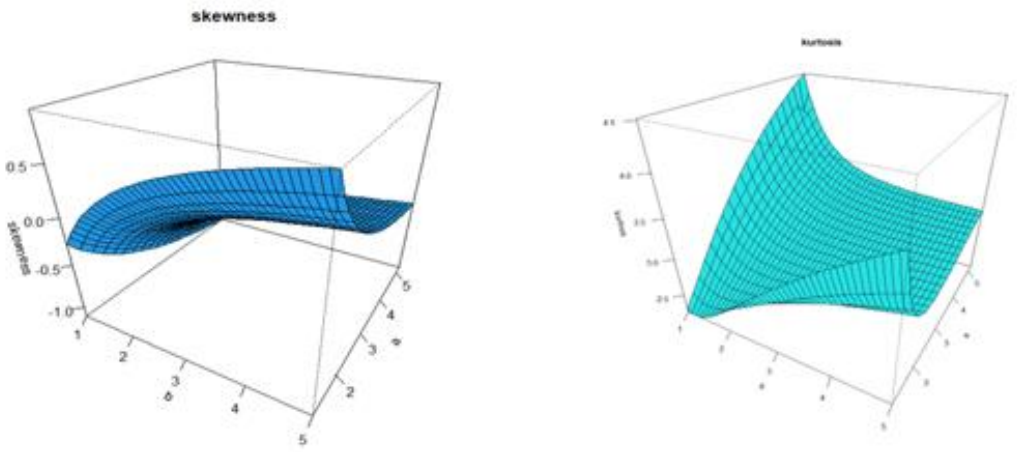


Figure 6. Plots of the GSK and MKU of the FExKw distribution.

We now provide a simple mixture for the FExKw density in terms of Kw densities. Based on Eq (4.3), the PDF of the FExKw takes the form

$$f(x) = \sum_{k=1}^{\infty} a_{k+1}(k+1)a\, b\, x^{a-1}(1 - x^a)^{b-1}[1 - (1 - x^a)^b]^k.$$

Applying binomial expansion to $[1 - (1 - x^a)^b]^k$, we have

$$f(x) = \sum_{k=1}^{\infty} \sum_{j=0}^{k} (-1)^j \binom{k}{j} a_{k+1}(k+1)a\, b\, x^{a-1}(1 - x^a)^{b(j+1)-1}.$$

The last equation can be expressed as

$$f(x) = \sum_{m=1}^{\infty} \delta_m \; g(x; a, mb), \quad 0 < x < 1,$$

where $\delta_m = \sum_{k=m}^{\infty} (-1)^{m-1} a_{k+1} \binom{k}{m-1} \frac{(k+1)}{m}$ and $g(x; a, mb) = a\, mb\, x^{a-1}(1-x^a)^{mb-1}$.

Based on the last equation, a simple formula for the rth raw moment of the FExKw distribution is as follows:

$$\mu_r' = E(X^r) = \sum_{m=1}^{\infty} \delta_m mb\, B\left(1 + \frac{r}{a}, mb\right). \tag{5.1}$$

Table 1 reports the values of μ_X obtained from the summation formula (SUM) and direct numerical integration (NUI) for different values of a and b, using several truncation levels H. The computations were performed in R. In the SUM approach, the infinite-series representation in (5.1) was truncated after H terms, whereas the NUI values were obtained by a direct numerical evaluation of the corresponding integral and used as a benchmark. In the numerical calculations based on the series representation in (5.1), the summation was truncated at several levels H in order to assess its convergence and numerical stability. In particular, the values reported in Table 1 correspond to $H = 5, 10, 15,$ and 20. The resulting SUM values were then compared with the corresponding values obtained by direct NUI. As shown in Table 1, the discrepancy between the two approaches decreases as H increases, and the approximation becomes numerically stable for sufficiently large truncation levels. This provides additional evidence for the accuracy and reliability of the series-based computation.

For $r = 1$, (5.1) reduces to the mean of the FExKw distribution, i.e., $\mu_1' = \mu_X$. It is given by

$$\mu_X = \sum_{m=1}^{\infty} \delta_m \, mb \, B\left(1 + \frac{1}{a}, mb\right).$$

The FExKw distribution's μ_x, variance (σ_x^2), skewness (ψ_1), and kurtosis (ψ_2) are numerically computed for specific values of a and b via R software. Table 2 displays the numerical values for all four measures. The table shows that μ_x and σ_x^2 are decreasing functions of b, while ψ_1 and ψ_2 are increasing function of b. It is also mentioned that ψ_1 can range in the interval $(-0.4404, 2.4814)$. The spread of ψ_2 is much larger ranging from 2.3419 to 11.0757.

Table 1. The values of μ_X generated by the SUM formula and NUI for various values of a and b at truncated H terms.

a	b	H	SUM	NUI
0.5	0.2	5	0.49238	0.86953
		10	0.68917	
		15	0.87143	
		20	0.87143	
	0.4	5	0.27300	0.69207
		10	0.50984	
		15	0.68601	
		20	0.68601	
	0.9	5	0.03969	0.40715
		10	0.24731	
		15	0.40287	
		20	0.40287	
0.8	0.2	5	0.57368	0.90724
		10	0.72767	
		15	0.91450	
		20	0.91450	
	0.4	5	0.38748	0.77340
		10	0.59215	
		15	0.77244	
		20	0.77244	
	0.9	5	0.15975	0.53482
		10	0.36714	
		15	0.53158	
		20	0.53158	
1.5	0.2	5	0.67411	0.94418
		10	0.76285	
		15	0.95691	
		20	0.95691	
	0.4	5	0.53708	0.85915
		10	0.67759	
		15	0.86542	
		20	0.86542	
	0.9	5	0.34790	0.69206
		10	0.51791	
		15	0.69391	
		20	0.69391	

Table 2. Numerical values for some measures of the FExKw distribution.

a	b	μ_x	σ_x^2	ψ_1	ψ_2
	1.5	0.2459	0.0454	1.1117	3.6259
	2	0.1750	0.0298	1.5451	5.2980
0.5	2.5	0.1309	0.0201	1.9032	7.1404
	3	0.1016	0.0139	2.2110	9.0810
	3.5	0.0812	0.0099	2.4814	11.0757
	1.5	0.3592	0.0493	0.5900	2.6044
	2	0.2814	0.0375	0.8993	3.3315
0.75	2.5	0.2289	0.0287	1.1339	4.0898
	3	0.1914	0.0223	1.3215	4.8338
	3.5	0.1635	0.0176	1.4766	5.5465
	1.5	0.4461	0.0469	0.2839	2.3419
	2	0.3690	0.0388	0.5420	2.7242
1	2.5	0.3144	0.0320	0.7285	3.1342
	3	0.2739	0.0266	0.8718	3.5307
	3.5	0.2426	0.0223	0.9865	3.9014
	1.5	0.5669	0.0378	−0.0784	2.3756
	2	0.4970	0.0344	0.1366	2.4719
1.5	2.5	0.4451	0.0308	0.2843	2.6241
	3	0.4049	0.0275	0.3933	2.7836
	3.5	0.3726	0.0247	0.4775	2.9357
	1.5	0.7001	0.0234	−0.4404	2.8166
	2	0.6453	0.0231	−0.2527	2.7010
2.5	2.5	0.6029	0.0222	−0.1292	2.6867
	3	0.5688	0.0211	−0.0410	2.7076
	3.5	0.5406	0.0201	0.0253	2.7410

5.2. Mathematical properties for the FExKw HRF

The HRF of the FExKw distribution can be studied through its behavior at the boundaries of the support. For small values of x (i.e. $x \to 0^+$), a series expansion yields

$$h(x;a,b) \sim C_0\, x^{2a-1}, \quad C_0 = 2pab^2 > 0.$$

Consequently, we have the following.

- For $0 < a < 1/2$, we have $2a - 1 < 0$, so $h(x)$ is decreasing in the neighborhood of the origin.
- For $a > 1/2$, we have $2a - 1 > 0$, so $h(x)$ is nondecreasing near the origin.

For large values of x (i.e., $x \to 1^-$), the HRF behaves as follows:

$$h(x;a,b) \sim \frac{ab}{1-x^a},$$

which is an increasing function of x and diverges to $+\infty$ as x approaches 1. Hence, the FExKw distribution is flexible enough to describe both aging (increasing) and bathtub-shaped hazard rates using only two shape parameters.

Proposition 1. The HRF of the FExKw distribution satisfies the following local properties:

(1) If $0 < a < 1/2$, then $h(x)$ is decreasing in the neighborhood of the origin.

(2) If $a > 1/2$, then $h(x)$ is nondecreasing in the neighborhood of the origin.

(3) For all $a, b > 0$, $h(x)$ is increasing for values of x sufficiently close to 1.

Proof: From the asymptotic expansion of the HRF near the origin, we have

$$h(x;a,b) \sim C_0 x^{2a-1},\ x \to 0^+,$$

where

$$C_0 = 2pab^2 > 0.$$

Differentiating the leading term gives

$$h'(x;a,b) \sim C_0(2a-1)x^{2a-2}, \qquad x \to 0^+.$$

Hence, if $0 < a < 1/2$, then $2a - 1 < 0$, and therefore,

$$h'(x) < 0$$

for values of x sufficiently close to 0. Thus, $h(x)$ is decreasing in the neighborhood of the origin.

If $a \geq 1/2$, then $2a - 1 \geq 0$, and therefore,

$$h'(x) \geq 0,$$

for x sufficiently close to 0. Thus, $h(x)$ is nondecreasing near the origin.

On the other hand, as $x \to 1^-$, the HRF satisfies

$$h(x;a,b) \sim \frac{ab}{1-x^a}.$$

Differentiating this asymptotic form, we obtain

$$h'(x;a,b) \sim \frac{a^2 b\, x^{a-1}}{(1-x^a)^2} > 0, \qquad x \to 1^-.$$

Therefore, $h(x)$ is increasing for values of x sufficiently close to 1. This completes the proof.

Remark 1. Proposition 1 describes the local behavior of the HRF near the boundaries of the support. In particular, for $0 < a < \frac{1}{2}$, the HRF decreases near $x = 0$ and increases near $x = 1$, suggesting the possibility of a bathtub-type pattern for suitable parameter values. This behavior is further illustrated numerically in the corresponding figures.

Remark 2. Proposition 1 also provides a systematic basis for comparing the HRF behavior of the proposed FExKw distribution with that of its baseline Kw counterpart. For the baseline Kw distribution, the HRF is given by

$$h_{Kw}(x) = \frac{abx^{a-1}}{1-x^a},\ 0 < x < 1,$$

which shows that its shape is mainly controlled by the parameter a. In particular, the baseline Kw HRF is increasing when $a \geq 1$, whereas for $0 < a < 1$, it exhibits a bathtub shape. By contrast, Proposition 1 shows, for the FExKw distribution, that

$$h(x) \sim C_0 x^{2a-1}, \qquad x \to 0^+.$$

Therefore, the local behavior near zero is determined by the threshold $a = 0.5$ rather than $a = 1$. In particular, when $0 < a < 0.5$, the HRF becomes unbounded near zero, which supports the appearance of bathtub-type behavior under suitable parameter settings. This analytical contrast shows that the proposed FEx-G transformation does not merely modify the baseline HRF quantitatively but changes its structural behavior in a meaningful way. Consequently, the proposed transformation enriches the shape flexibility of the baseline distribution without introducing additional parameters. Similar comparative analyses may also be developed for other FEx-G submodels, further confirming that the proposed generator can systematically expand the range of attainable HRF patterns beyond those of the corresponding baseline families.

5.3. Mean residual life function

The mean residual life (MRL) is a reliability measure that is the average remaining lifetime of a component (or individual) after it has survived up to time t. The main value of the MRL is that it describes the whole distribution of the remaining (residual) failure time beyond t, whereas the HRF focuses on the instantaneous failure tendency over a very small interval just after t.

Formally, for a lifetime RV X, the MRL at time t is defined as the conditional expectation of the remaining life

$$\mu(t) = E(X - t \mid X > t).$$

Using the SF $S(t) = P(X > t)$, and noting that the support of X is $(0,1)$ (as in the Kw baseline), this can be written equivalently as

$$\mu(t) = \frac{1}{S(t)} \int_t^1 (x - t)\, f(x)\, dx.$$

By integration by parts, we obtain

$$\mu(t) = \frac{1}{S(t)} \int_t^1 S(x)\, dx, \quad 0 \le t < 1.$$

Notice that at $t = 0$, the MRL reduces to the mean lifetime, i.e., $\mu(0) = E(X)$.
There is also a useful link between the HRF $h(t)$ and the MRL. If $\mu(t)$ is differentiable, then

$$h(t) = \frac{\mu'(t)}{\mu(t)} + \frac{1}{\mu(t)},$$

where $\mu'(t)$ denotes the derivative of $\mu(t)$ with respect to t. This relationship shows that the lifetime distribution can be characterized through $\mu(t)$ together with $h(t)$.

5.4. MRL of the FExKw distribution

Using the mixture representation of the FExKw density, the FIM can be derived in a straightforward way. From the expansion

$$f(x) = \sum_{m=1}^{\infty} \delta_m \; g(x; a, mb), \quad 0 < x < 1,$$

where $\delta_m = \sum_{k=m}^{\infty} (-1)^{m-1} a_{k+1} \binom{k}{m-1} \frac{(k+1)}{m}$ and $g(x; a, mb) = a\, mb\, x^{a-1}(1 - x^a)^{mb-1}$.

The FIM is defined by

$$\varphi_1(t) = \int_0^t x\, f(x)\, dx.$$

Substituting the mixture form above into the integral gives

$$\varphi_1(t) = \int_0^t x \sum_{m=1}^{\infty} \delta_m \; g(x; a, mb)\, dx.$$

Under standard regularity conditions, summation and integration can be interchanged, yielding

$$\varphi_1(t) = \sum_{m=1}^{\infty} \delta_m \int_0^t x\, g(x; a, mb)\, dx.$$

Now, using the expression of $g(x; a, mb)$, we obtain

$$\varphi_1(t) = \sum_{m=1}^{\infty} \delta_m \; a\, mb \int_0^t x^a\, (1 - x^a)^{mb-1}\, dx.$$

Next, apply the transformation $u = x^a$ so that $dx = \frac{1}{a} u^{1/a-1} du$, and the integral reduces to

$$\varphi_1(t) = \sum_{m=1}^{\infty} \delta_m \; mb \int_0^{t^a} u^{1/a}\, (1 - u)^{mb-1}\, du.$$

Recognizing the last integral as the incomplete BF, the FIM of the FExKw model is

$$\varphi_1(t) = \sum_{m=1}^{\infty} \delta_m \, mb \, B_{t^a}\left(1 + \frac{1}{a}, mb\right). \tag{5.2}$$

The MRL of X is written as

$$\mu(t) = \frac{\mu_1' - \varphi_1(t)}{S(t)} - t, \tag{5.3}$$

where $S(t) = 1 - F(t)$ denotes the SF of the FExKw distribution and μ_1' is the mean obtained from Eq (5.1).

The MRL of X follows by inserting $\varphi_1(t)$ in Eq (5.2), as follows:

$$\mu(t) = \frac{1}{S(t)}\left[\mu_1' - \sum_{m=1}^{\infty} \delta_m \, mb \, B_{t^a}\left(1 + \frac{1}{a}, mb\right)\right] - t. \tag{5.4}$$

Computing $\mu(t)$ directly from Eq (5.4) is not very convenient in practice. Instead, we derive a simpler asymptotic approximation for $\mu(t)$ that becomes accurate when t is sufficiently close to 1. This leads to the following proposition.

Proposition 2. For sufficiently large values of t, i.e., as $t \to 1^-$, we have

$$\mu(t) \sim \frac{1-t}{b+1}. \tag{5.5}$$

Proof:

$$\mu(t) = \frac{1}{S(t)} \int_t^1 S(x)\, dx = \int_0^{1-t} \frac{S(t+u)}{S(t)}\, du,$$

where $S(x) = \frac{1}{\exp(1)-1}\{\exp[H(x)] - 1\}$ and $H(x) = (1 - x^a)^{b[1-(1-x^a)^b]}$.

Let $x \to 1^-$, and let $y = 1 - x^a$, so $y \downarrow 0$. Then, we have

$$\ln H(x) = b(1 - y^b)\ln y = b \ln y - by^b \ln y.$$

Since $y^b \ln y \to 0$ as $y \to 0^+$, we get $\ln H(x) = b \ln y$ and $H(x) = y^b$, and hence, $H(x) \to 0$ and $\exp[H(x)] - 1 \sim H(x) \sim (1 - x^a)^b$ and $x \to 1^-$.

Therefore,

$$S(x) \sim \frac{1}{e-1}(1 - x^a)^b, \qquad x \to 1^-.$$

Using $1 - x^a = 1 - (1 - (1 - x))^a \sim a(1 - x)$ as $x \to 1^-$.
We obtain the simpler form

$$S(x) \sim K(1 - x)^b, K = \frac{a^b}{e-1} > 0, x \to 1^-.$$

Now,

$$\mu(t) = \int_0^{1-t} \frac{S(t+u)}{S(t)}\, du.$$

Let $d(t) = 1 - t$ and set $u = d(t)y,\ 0 \le y \le 1$. Then

$$\mu(t) = d(t) \int_0^1 \frac{S(1-d(t)(1-y))}{S(1-d(t))}\, dy.$$

As $t \to 1^-,\ d(t) \downarrow 0$, using $S(x) \sim K(1-x)^b$, and hence, we have

$$\frac{S(1-d(t)(1-y))}{S(1-d(t))} \sim \left(\frac{d(t)(1-y)}{d(t)}\right)^b = (1-y)^b.$$

Hence,

$$\mu(t) \sim d(t) \int_0^1 (1-y)^b\, dy = d(t)\ \frac{1}{b+1} = \frac{1-t}{b+1},\ t \to 1^-.$$

Table 3 presents selected values of the MRL function obtained both from the asymptotic approximation in (5.5) and from numerical integration, for several combinations of the parameters a and b and different time points. As t increases, the two sets of values remain close to each other, indicating that the approximation in (5.5) provides results that are increasingly consistent with those produced by numerical integration.

Table 3. MRL of the FExKw distribution for different parameter values.

a	b	t	Equation (5.4)	Equation (5.5)
0.5	0.5	0.2	0.48146	0.53333
		0.5	0.29644	0.33333
		0.7	0.17845	0.20000
		0.9	0.06092	0.06666
0.5	2	0.2	0.17947	0.26666
		0.5	0.13939	0.16666
		0.7	0.09190	0.10000
		0.9	0.03269	0.03333
2	0.5	0.2	0.65762	0.53333
		0.5	0.37110	0.33333
		0.7	0.20274	0.20000
		0.9	0.06170	0.06666
2	2	0.2	0.38794	0.26666
		0.5	0.17314	0.16666
		0.7	0.09452	0.10000
		0.9	0.03266	0.03333

5.5. Shapes of MRL and changing points

Lemma 1. Let $X \sim \text{FExKw}(a, b)$. Then all positive moments of X are finite. In particular, the mean exists and is finite.

Proof: For any $r > 0$, the rth moment of X can be written as

$$\mu'_r = E(X^r) = r \int_0^1 x^{r-1} S(x)\, dx,$$

where $0 < S(x) \leq 1$ for all $0 < x < 1$, we have

$$\mu'_r \leq r \int_0^1 x^{r-1}\, dx = 1 < \infty.$$

Hence, all positive moments of the FExKw distribution are finite. In particular, the mean exists and satisfies

$$\mu'_1 = E(X) < \infty.$$

This completes the proof.

Remark 3. For $X \sim \text{FExKw}(a, b)$ with $0 < a < 1/2$, the boundary behavior of the HRF, together with the finiteness of the mean established in Lemma 1, is consistent with the possibility of an upside-down bathtub shape for the MRL under suitable parameter settings. This interpretation is also supported by the numerical illustrations in Figure 7.

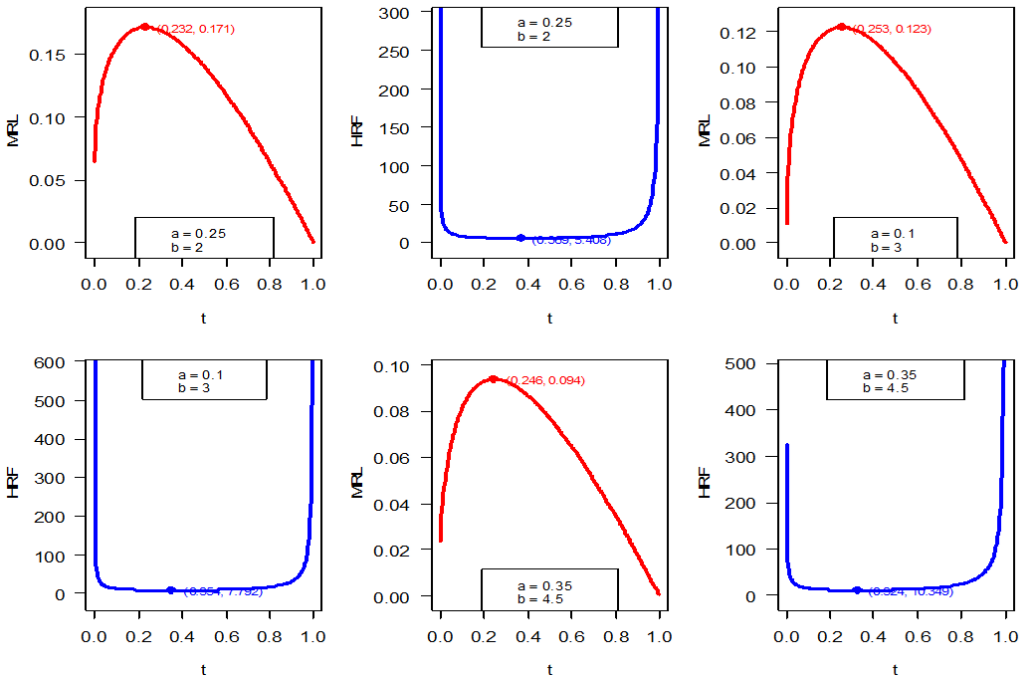


Figure 7. Plots of the MRL and HRF with their changing points.

According to Mi [31], under appropriate regularity conditions, such the HRF's behavior together with a finite mean supports the possibility of an upside-down bathtub shape for the MRL function. Therefore, the MRL of the FExKw distribution is capable of exhibiting an upside-down bathtub shape.

Proposition 3. The asymptotic behavior of the HRF $h(t)$ and the reciprocal of the MRL $\mu(t)$ are equivalent as $t \to 1^-$.

$$\lim_{t\to 1^-} h(t) = \lim_{t\to 1^-} \frac{1}{\mu(t)} = +\infty \quad \text{and} \quad \lim_{t\to 1^-} \frac{h(t)}{1/\mu(t)} = \frac{b}{b+1}.$$

Proof:

$$h(t) = \frac{\mu'(t)}{\mu(t)} + \frac{1}{\mu(t)}. \tag{5.6}$$

$$\frac{d}{dt}\ln \mu(t) = \frac{\mu'(t)}{\mu(t)} = h(t) - \frac{1}{\mu(t)}.$$

From Eq (5.5), we immediately get

$$\frac{1}{\mu(t)} \sim \frac{b+1}{1-t}, \ \mu'(t) \sim -\frac{1}{b+1}, \ t \to 1^-.$$

Hence,

$$\frac{\mu'(t)}{\mu(t)} \sim \frac{-\frac{1}{b+1}}{(1-t)/(b+1)} = -\frac{1}{1-t}, \ t \to 1^-.$$

Substituting into (5.6), we have

$$h(t) = \frac{\mu'(t)}{\mu(t)} + \frac{1}{\mu(t)} \sim \left(-\frac{1}{1-t}\right) + \frac{b+1}{1-t} = \frac{b}{1-t}, \ t \to 1^-.$$

Thus,

$$h(t) \sim \frac{b}{1-t}, \ \frac{1}{\mu(t)} \sim \frac{b+1}{1-t}.$$

Therefore, both $h(t)$ and $1/\mu(t)$ blow up to $+\infty$ at the same rate (up to the constant factor $b/(b+1)$). In other words, the asymptotic behavior of the HRF and the reciprocal of MRL for the FExKw distribution is essentially the same as $t \to 1^-$.

Figure 7 compares the MRL and HRF curves for three choices of (a, b). For $(0.25, 2)$, the MRL rises quickly to a peak (around $t \approx 0.232$) and then decreases toward zero as t approaches 1, while the HRF shows the usual bathtub pattern that is very high near $t = 0$, lowest in the middle, and increasing sharply again close to $t = 1$. For $(0.1, 3)$, the MRL also peaks early (about $t \approx 0.253$), and the HRF is again bathtub-shaped, with its minimum occurring a larger t than the MRL's peak. For $(0.35, 4.5)$, the MRL remains unimodal with a peak near $t \approx 0.246$, and the HRF is strongly bathtub-shaped with a sharp rise as $t \to 1^-$.

6. Estimation of the FExKw parameters

This section uses nine methods to estimate FExKw parameters, including the least squares (LS), maximum product of spacing (MPS), moment method (MM), maximum likelihood (ML), weighted least squares (WLS), Cramér–von Mises (CVM), percentiles (PC), Anderson–Darling (AD), and right-tail Anderson–Darling (RTAD).

Assume that $x_1, \ldots, x_n$ is a random sample from the FExKw distribution with the parameters a and b. Consider the associated order statistics as $x_{1:n} < x_{2:n} < \cdots < x_{n:n}$.

The log-likelihood function has the following form:

$$\ell = n\log p + n\log a + n\log b + (a-1)\sum_{i=1}^{n}\log x_i + \sum_{i=1}^{n}\left(2b - 1 - b\,{k_i}^{b}\right)\log(k_i) +$$

$$\sum_{i=1}^{n}\log\left(\left({k_i}^{-b} - 1\right) - b\log(k_i)\right) - \sum_{i=1}^{n} 1 - {k_i}^{b\left(1-{k_i}^{b}\right)},$$

where $k_i = 1 - {x_i}^{a}$. To obtain the ML estimators (MLEs) of a and b, maximize the last equation with respect to a and b, or solve the nonlinear equations

$$\frac{\partial \ell}{\partial a} = \frac{n}{a} + \sum_{i=1}^{n}\log x_i + b^2{k_i}^{b-1}({x_i}^{a}\log x_i)\log(k_i) - \left(2b - 1 - b\,{k_i}^{b}\right)\left(\frac{{x_i}^{a}\log x_i}{k_i}\right) +$$

$$\frac{1}{\left[\left({k_i}^{-b}-1\right)-b\log(k_i)\right]}\left[b{k_i}^{-b-1}({x_i}^{a}\log x_i) + b\left(\frac{{x_i}^{a}\log x_i}{k_i}\right)\right] +$$

$${k_i}^{b\left(1-{k_i}^{b}\right)}\left\{\left[b^2{k_i}^{b-1}({x_i}^{a}\log x_i)\right]\log k_i + \left[b\left(1-{k_i}^{b}\right)\right]\left(\frac{{x_i}^{a}\log x_i}{k_i}\right)\right\} = 0,$$

and

$$\frac{\partial \ell}{\partial b} = \frac{n}{b} + \sum_{i=1}^{n}\left[2 - {k_i}^{b} - b{k_i}^{b}\log(k_i)\right]\log k_i - \frac{{k_i}^{-b}\log(k_i) - \log(k_i)}{\left({k_i}^{-b}-1\right)-b\log(k_i)} + {k_i}^{b\left(1-{k_i}^{b}\right)}\left[\left(1-{k_i}^{b}\right) -\right.$$

$$\left. b{k_i}^{b}\log(k_i)\right]\log(k_i) = 0.$$

Additionally, ML method can be achieved via various programs, including SAS (PROC NLMIXED), Mathematica, and R (optim function).

The MM estimators (MMEs) for a and b can be obtained by equating the sample moments $m_r = \frac{1}{n}\sum_{i=1}^{n} x_i^r$ to their corresponding theoretical moments $\mu_r(a,b) = \int_0^1 x^r f(x;a,b)\,dx$ for $r = 1,2,3,\cdots,j$. Then solve the nonlinear system $\mu_r(a,b) = m_r$ or minimize the function with respect to a and b $\sum_{r=1}^{j}(\mu_r(a,b) - m_r)^2$.

The LS estimators (LSEs) and WLS estimators (WLSEs) of the FExKw parameters a and b can be calculated through minimizing the following function with respect to a and b:

$$\mathrm{V}(a,b) = \sum_{i=1}^{n} v_i\left\{\left[p\,\left(1 - \exp\left\{-\left[1 - {k_{i:n}}^{b\left(1-{k_{i:n}}^{b}\right)}\right]\right\}\right)\right] - \frac{i}{n+1}\right\}^2,$$

where $k_{i:n} = 1 - x_{i:n}^{a}$. In the LS approach, $v_i = 1$; in the WLS approach, $v_i = \frac{(n+1)^2(n+2)}{[i(n-i+1)]}$. Moreover, the LSEs and WLSEs can also be determined by solving the following nonlinear equations:

$$\sum_{i=1}^{n} v_i\left\{\left[p\,\left(1 - \exp\left\{-\left[1 - {k_{i:n}}^{b\left(1-{k_{i:n}}^{b}\right)}\right]\right\}\right)\right] - \frac{i}{n+1}\right\}\Delta_s(x_{i:n}^{a}|a,b) = 0,\ \ s = 1,2,$$

where

$$\Delta_1(x_{i:n}^a|a,b) = \frac{\partial \ell}{\partial a}\mathrm{F}(x_{i:n}|a,b) = p\ \left(1-\exp\left\{-\left[1-{k_{i:n}}^{b\left(1-{k_{i:n}}^{b}\right)}\right]\right\}\right){k_{i:n}}^{b\left(1-{k_{i:n}}^{b}\right)}$$

$$\times\left[b^2{k_{i:n}}^{b-1}x_{i:n}^a\log(x_{i:n})\log(k_{i:n}) - \frac{b\left(1-{k_{i:n}}^{b}\right)x_{i:n}^a\log(x_{i:n})}{k_{i:n}}\right], \tag{6.1}$$

and

$$\Delta_2(x_{i:n}^a|a,b) = \frac{\partial \ell}{\partial b}F(x_{i:n}|a,b)\ = p{k_{i:n}}^{b\left(1-{k_{i:n}}^{b}\right)}\left(1-\exp\left\{-\left[1-{k_{i:n}}^{b\left(1-{k_{i:n}}^{b}\right)}\right]\right\}\right)$$

$$\times\left[1-{k_{i:n}}^{b}-b{k_{i:n}}^{b}\log(k_{i:n})\right]\log(k_{i:n}). \tag{6.2}$$

Cheng and Amin [32, 33] showed that the MPS method is a good alternative to the ML approach. A random sample of size n from the FExKw distribution with uniform spacings, denoted D_i, is defined as

$$D_i = F(x_{i:n}|a,b) - F(x_{i-1:n}|a,b),$$

where $F(x_{0:n}|a,b) = 0, F(x_{n+1:n}|a,b) = 1$, and $\sum_{i=1}^{n+1} D_i(a,b) = 1$.

The MPS estimators (MPSEs) of the FExKw parameters can be obtained by maximizing

$$\mathrm{G}(a,b) = \frac{1}{n+1}\sum_{i=1}^{n+1}\log D_i(a,b),$$

with respect to a and b. Additionally, the MPSEs of the FExKw parameters can be derived by solving

$$\frac{1}{n+1}\sum_{i=1}^{n+1}\frac{1}{D_i(a,b)}[\Delta_s(x_{i:n}|a,b) - \Delta_s(x_{i-1:n}|a,b)] = 0,$$

where $\Delta_s(x_{i:n}|a,b) = 0$ are defined in (6.1) and (6.2) for $s = 1,2$.

The unknown parameters of the FExKw distribution are approximated by the PC technique [34], which equals the PC values of the sample and the population. Let $u_i = i/(n+1)$ be an unbiased estimator of $F(x_{i:n}|a,b)$. After that, the PC estimators (PCEs) of the FExKw parameters are acquired by minimizing the function

$$P(a,b) = \sum_{i=1}^{n}\left(x_{i:n} - \left\{1-\left[1+\log\left(1-\frac{u_i}{p}\right)\right]^{\frac{1}{b\left(1-k^b\right)}}\right\}^{\frac{1}{a}}\right),$$

with respect to a and b, where $p = \mathrm{e}/(\mathrm{e}-1)$.

The CVM estimators (CVMEs) were discussed by Cramér [35] and von Mises [36]. These estimators can be determined through the difference between the estimated CDF and the empirical CDF. The CVMEs for the FExKw parameters are calculated by minimizing

$$C(a,b) = \frac{1}{12n} + \sum_{i=1}^{n}\left\{\left[p\ \left(1-\exp\left\{-\left[1-{k_{i:n}}^{b\left(1-{k_{i:n}}^{b}\right)}\right]\right\}\right)\right] - \frac{2i-1}{2n}\right\}^2.$$

Furthermore, the CVMEs concluded by solving the nonlinear equations

$$\sum_{i=1}^{n}\left\{\left[p\left(1-\exp\left\{-\left[1-k_{i:n}{}^{b\left(1-k_{i:n}{}^{b}\right)}\right]\right\}\right)\right]-\frac{2i-1}{2n}\right\}\Delta_s(x_{i:n}|a,b)=0,$$

where $\Delta_s(x_{i:n}|a,b)=0$ are defined in (6.1) and (6.2) for $s=1,2$.

An additional type of minimum distance estimator is the AD. The AD estimators (ADEs) of the FExKw parameters can be determined by minimizing

$$A(a,b)=-n-\frac{1}{n}\sum_{i=1}^{n}(2i-1)[\log F(x_{i:n}|a,b)+\log\bar{F}(x_{n+1-i:n}|a,b)].$$

The ADEs can also be calculated by solving the nonlinear equations

$$\sum_{i=1}^{n}(2i-1)\left[\frac{\Delta_s(x_{i:n}|a,b)}{F(x_{i:n}|a,b)}-\frac{\Delta_j(x_{n+1-i:n}|a,b)}{S(x_{n+1-i:n}|a,b)}\right]=0.$$

The RTAD estimators (RTADEs) for the FExKw parameters a and b can be calculated by minimizing the function

$$R(a,b)=\frac{n}{2}-2\sum_{i=1}^{n}F(x_{i:n}|a,b)-\frac{1}{n}\sum_{i=1}^{n}(2i-1)\log\bar{F}(x_{n+1-i:n}|a,b).$$

7. Simulation analysis

In this section, we use a simulation study to evaluate and explore the effectiveness of all estimation methods of the FExKw parameters. We generate 5000 samples from the FExKw distribution for various sample sizes of $n=\{20,50,100,250\}$ and various parametric values of $a=(0.5,0.2,1.2,1.7,2.3,1.3,2.5,3.5,0.4,0.7,0.8)$ and $b=(0.5,0.5,3.5,2.5,2,0.5,2.5,0.7,1.25,0.9,1.5)$. For every estimate, we compute the average mean square error (MSE), average absolute bias (AB), and average mean relative error (MRE). The optimal estimation method for the FExKw parameters was identified by evaluating these measures according to their partial and overall rankings.

Tables 4–14 present the simulation study's results, which include the AB, MSE, and MRE of the MLEs, LSEs, WLSEs, MPSEs, PCEs, CVMEs, ADEs, RTADEs, and MMEs. Additionally, these tables include $\sum Ranks$, that is, a partial total of the ranks of each column in a given sample size, and superscripts, which show each estimator's rank among all estimators. Tables 4–14 demonstrate that all estimators show consistency, with a decreasing AB, MSE, and MRE when the sample size increases. Table 15 shows that the MM is the best estimation method because it has low AB, MSE, and MRE values. RTAD and MPS are the second-best estimation methods. It also shows the overall position of the estimators, which lets us determine if MMEs is better. According to Table 15, the estimators are ranked from best to worst for each parameter combination as MMEs, RTADEs, MPSEs, MLEs, WLSEs, PCEs, ADEs, LSEs, and CVMEs.

Table 4. Simulation results for the nine estimation methods for $a = 0.5$ and $b = 0.5$.

n	Est.	Par.	MLEs	LSEs	WLSEs	MPSEs	PCEs	CVMEs	ADEs	RTADEs	MMEs
20	AB	$\hat{a}$	0.19304^{6}	0.20471^{7}	0.19238^{5}	0.16269^{2}	0.18276^{4}	0.24418^{8}	0.24474^{9}	0.16838^{3}	0.11846^{1}
		$\hat{b}$	0.12341^{6}	0.12522^{7}	0.11905^{4}	0.10510^{3}	0.12073^{5}	0.15229^{9}	0.13689^{8}	0.09924^{2}	0.08076^{1}
	MSE	$\hat{a}$	0.07555^{6}	0.08167^{7}	0.07228^{5}	0.04155^{3}	0.05787^{4}	0.13826^{8}	0.14007^{9}	0.02835^{2}	0.01403^{1}
		$\hat{b}$	0.03086^{6}	0.03126^{7}	0.02632^{5}	0.01797^{3}	0.02556^{4}	0.05586^{9}	0.04177^{8}	0.00985^{2}	0.00652^{1}
	MRE	$\hat{a}$	0.38607^{6}	0.40942^{7}	0.38476^{5}	0.32538^{2}	0.36552^{4}	0.48835^{8}	0.48948^{9}	0.33675^{3}	0.23691^{1}
		$\hat{b}$	0.24683^{6}	0.25045^{7}	0.23809^{4}	0.21020^{3}	0.24147^{5}	0.30458^{9}	0.27377^{8}	0.19848^{2}	0.16153^{1}
	$\sum$ Ranks		36^{6}	42^{7}	28^{5}	16^{3}	26^{4}	$51^{8.5}$	$51^{8.5}$	14^{2}	6^{1}
50	AB	$\hat{a}$	0.10330^{3}	0.12182^{7}	0.11417^{5}	0.10055^{2}	0.11469^{6}	0.13230^{8}	0.13973^{9}	0.10958^{4}	0.06727^{1}
		$\hat{b}$	0.06667^{4}	0.07520^{6}	0.07097^{5}	0.06380^{3}	0.07684^{7}	0.08146^{9}	0.07877^{8}	0.06159^{2}	0.04935^{1}
	MSE	$\hat{a}$	0.01938^{4}	0.02539^{7}	0.02222^{6}	0.01568^{3}	0.02104^{5}	0.03136^{8}	0.03579^{9}	0.01201^{2}	0.00453^{1}
		$\hat{b}$	0.00790^{4}	0.00959^{7}	0.00852^{5}	0.00641^{3}	0.00947^{6}	0.01187^{9}	0.01106^{8}	0.00379^{2}	0.00244^{1}
	MRE	$\hat{a}$	0.20660^{3}	0.24364^{7}	0.22833^{5}	0.20109^{2}	0.22938^{6}	0.26461^{8}	0.27946^{9}	0.21916^{4}	0.13454^{1}
		$\hat{b}$	0.13333^{4}	0.15039^{6}	0.14194^{5}	0.12759^{3}	0.15369^{7}	0.16293^{9}	0.15754^{8}	0.12318^{2}	0.09871^{1}
	$\sum$ Ranks		22^{4}	40^{7}	31^{5}	$16^{2.5}$	37^{6}	$51^{8.5}$	$51^{8.5}$	$16^{2.5}$	6^{1}
100	AB	$\hat{a}$	0.06991^{2}	0.08545^{7}	0.07783^{5}	0.07119^{3}	0.08149^{6}	0.08748^{8}	0.09449^{9}	0.07719^{4}	0.04186^{1}
		$\hat{b}$	0.04554^{4}	0.05295^{6}	0.04961^{5}	0.04448^{2}	0.05329^{7}	0.05487^{9}	0.05351^{8}	0.04495^{3}	0.03324^{1}
	MSE	$\hat{a}$	0.00847^{4}	0.01171^{7}	0.00996^{5}	0.00786^{3}	0.01052^{6}	0.01270^{8}	0.01527^{9}	0.00596^{2}	0.00175^{1}
		$\hat{b}$	0.00353^{4}	$0.00451^{6.5}$	0.00403^{5}	0.00314^{3}	$0.00451^{6.5}$	0.00509^{9}	0.00478^{8}	0.00202^{2}	0.00111^{1}
	MRE	$\hat{a}$	0.13982^{2}	0.17090^{7}	0.15565^{5}	0.14239^{3}	0.16299^{6}	0.17497^{8}	0.18898^{9}	0.15437^{4}	0.08372^{1}
		$\hat{b}$	0.09107^{4}	0.10590^{6}	0.09922^{5}	0.08895^{2}	0.10658^{7}	0.10975^{9}	0.10701^{8}	0.08989^{3}	0.06649^{1}
	$\sum$ Ranks		20^{4}	39.5^{7}	30^{5}	13^{2}	38.5^{6}	$51^{8.5}$	$51^{8.5}$	18^{3}	6^{1}
250	AB	$\hat{a}$	0.04104^{3}	0.05362^{7}	0.04780^{4}	0.04031^{2}	0.05252^{6}	0.05497^{8}	0.05781^{9}	0.05038^{5}	0.02105^{1}
		$\hat{b}$	0.02631^{3}	0.03351^{7}	0.03041^{5}	0.02555^{2}	0.03454^{9}	0.03352^{8}	0.03330^{6}	0.02858^{4}	0.02254^{1}
	MSE	$\hat{a}$	0.00303^{4}	0.00458^{7}	0.00365^{5}	0.00279^{3}	0.00431^{6}	0.00483^{8}	0.00541^{9}	0.00254^{2}	0.00044^{1}
		$\hat{b}$	0.00123^{4}	0.00177^{6}	0.00146^{5}	0.00113^{3}	0.00189^{9}	0.00181^{8}	0.00178^{7}	0.00082^{2}	0.00051^{1}
	MRE	$\hat{a}$	0.08208^{3}	0.10724^{7}	0.09559^{4}	0.08062^{2}	0.10503^{6}	0.10994^{8}	0.11562^{9}	0.10075^{5}	0.04209^{1}
		$\hat{b}$	0.05262^{3}	0.06702^{7}	0.06083^{5}	0.05110^{2}	0.06907^{9}	0.06703^{8}	0.06660^{6}	0.05716^{4}	0.04507^{1}
	$\sum$ Ranks		20^{3}	41^{6}	28^{5}	14^{2}	45^{7}	48^{9}	46^{8}	22^{4}	6^{1}

Table 5. Simulation results for the nine estimation methods for $a = 0.2$ and $b = 0.5$.

n	Est.	Par.	MLEs	LSEs	WLSEs	MPSEs	PCEs	CVMEs	ADEs	RTADEs	MMEs
20	AB	$\hat{a}$	0.07599^{4}	0.08248^{6}	0.07910^{5}	0.06316^{2}	0.09089^{7}	0.09457^{8}	0.09773^{9}	0.07307^{3}	0.06602^{1}
		$\hat{b}$	0.12259^{5}	0.12735^{6}	0.12115^{4}	0.10225^{2}	0.13184^{7}	0.14540^{9}	0.13449^{8}	0.10281^{3}	0.09338^{1}
	MSE	$\hat{a}$	0.01247^{4}	0.01330^{6}	0.01319^{5}	0.00667^{3}	0.01401^{7}	0.02065^{8}	0.02308^{9}	0.00534^{2}	0.00436^{1}
		$\hat{b}$	0.03202^{6}	0.03250^{7}	0.03006^{4}	0.01816^{3}	0.03044^{5}	0.04707^{9}	0.03802^{8}	0.01057^{2}	0.00872^{1}
	MRE	$\hat{a}$	0.37995^{4}	0.41239^{6}	0.39551^{5}	0.31581^{1}	0.45445^{7}	0.47286^{8}	0.48867^{9}	0.36535^{3}	0.33008^{2}
		$\hat{b}$	0.24518^{5}	0.25469^{6}	0.24230^{4}	0.20451^{2}	0.26369^{7}	0.29080^{9}	0.26897^{8}	0.20562^{3}	0.18675^{1}
	$\sum$ Ranks		28^{5}	37^{6}	27^{4}	13^{2}	40^{7}	$51^{8.5}$	$51^{8.5}$	16^{3}	7^{1}
50	AB	$\hat{a}$	0.03887^{2}	0.04944^{6}	0.04555^{5}	0.03545^{1}	0.05826^{9}	0.05337^{7}	0.05411^{8}	0.04514^{4}	0.04182^{3}
		$\hat{b}$	0.06258^{4}	0.07496^{6}	0.07206^{5}	0.05864^{1}	0.08197^{8}	0.08211^{9}	0.07622^{7}	0.06167^{2}	0.06187^{3}
	MSE	$\hat{a}$	0.00298^{4}	0.00414^{6}	0.00360^{5}	0.00214^{3}	0.00553^{9}	0.00516^{7}	0.00533^{8}	0.00204^{2}	0.00175^{1}
		$\hat{b}$	0.00745^{4}	0.00955^{6}	0.00881^{5}	0.00579^{3}	0.01130^{8}	0.01199^{9}	0.01001^{7}	0.00380^{1}	0.00383^{2}
	MRE	$\hat{a}$	0.19436^{2}	0.24721^{6}	0.22777^{5}	0.17726^{1}	0.29132^{8}	0.26685^{9}	0.27053^{8}	0.22571^{4}	0.20908^{3}
		$\hat{b}$	0.12515^{4}	0.14992^{6}	0.14413^{5}	0.11729^{1}	0.16395^{8}	0.16422^{9}	0.15245^{7}	0.12333^{2}	0.12373^{3}
	$\sum$ Ranks		20^{4}	36^{6}	30^{5}	10^{1}	$50^{8.5}$	$50^{8.5}$	45^{7}	$15^{2.5}$	$15^{2.5}$
100	AB	$\hat{a}$	0.02474^{2}	0.03395^{6}	0.03122^{5}	0.02235^{1}	0.04165^{9}	0.03580^{7}	0.03738^{8}	0.03014^{4}	0.02959^{3}
		$\hat{b}$	0.03999^{2}	0.05290^{6}	0.04949^{5}	0.03705^{1}	0.05839^{9}	0.05398^{8}	0.05346^{7}	0.04244^{3}	0.04393^{4}
	MSE	$\hat{a}$	0.00124^{4}	0.00192^{6}	0.00160^{5}	0.00095^{3}	0.00275^{9}	0.00212^{7}	0.00237^{8}	0.00091^{2}	0.00088^{1}
		$\hat{b}$	0.00327^{4}	0.00465^{6}	0.00403^{5}	0.00257^{3}	0.00546^{9}	0.00487^{8}	0.00477^{7}	0.00180^{1}	0.00193^{2}
	MRE	$\hat{a}$	0.12371^{2}	0.16977^{6}	0.15609^{5}	0.11174^{1}	0.20827^{9}	0.17899^{7}	0.18692^{8}	0.15071^{4}	0.14794^{3}
		$\hat{b}$	0.07997^{2}	0.10579^{6}	0.09899^{5}	0.07410^{1}	0.11679^{9}	0.10795^{8}	0.10692^{7}	0.08488^{3}	0.08786^{4}
	$\sum$ Ranks		16^{2}	36^{6}	30^{5}	10^{1}	54^{9}	$45^{7.5}$	$45^{7.5}$	$17^{3.5}$	$17^{3.5}$
250	AB	$\hat{a}$	0.01140^{2}	0.02176^{6}	0.01906^{4}	0.01080^{1}	0.02661^{9}	0.02201^{7}	0.02298^{8}	0.02001^{5}	0.01884^{3}
		$\hat{b}$	0.01839^{2}	0.03345^{7}	0.02992^{5}	0.01804^{1}	0.03745^{9}	0.03376^{8}	0.03329^{6}	0.02719^{4}	0.02715^{3}
	MSE	$\hat{a}$	0.00034^{2}	0.00075^{6}	0.00059^{5}	0.00029^{1}	0.00111^{9}	0.00079^{7}	0.00085^{8}	0.00040^{4}	0.00035^{3}
		$\hat{b}$	0.00089^{4}	0.00178^{7}	0.00145^{5}	0.00080^{3}	0.00220^{9}	0.00182^{8}	0.00175^{6}	$0.00074^{1.5}$	$0.00074^{1.}$
	MRE	$\hat{a}$	0.05699^{2}	0.10880^{6}	0.09532^{4}	0.05402^{1}	0.13303^{9}	0.11004^{7}	0.11489^{8}	0.10003^{5}	0.09418^{3}
		$\hat{b}$	0.03679^{2}	0.06689^{7}	0.05983^{5}	0.03608^{1}	0.07490^{9}	0.06752^{8}	0.06657^{6}	0.05438^{4}	0.05430^{3}
	$\sum$ Ranks		14^{2}	39^{6}	28^{5}	8^{1}	54^{9}	45^{8}	42^{7}	23.5^{4}	16.5^{3}

Table 6. Simulation results for the nine estimation methods for $a = 1.2$ and $b = 3.5$.

n	Est.	Par.	MLEs	LSEs	WLSEs	MPSEs	PCEs	CVMEs	ADEs	RTADEs	MMEs
20	AB	$\hat{a}$	0.24155^{4}	0.27311^{8}	0.24782^{6}	0.23656^{3}	0.24573^{5}	0.27998^{9}	0.27310^{7}	0.21785^{2}	0.20934^{1}
		$\hat{b}$	1.59527^{5}	1.64249^{7}	1.62478^{6}	1.16810^{3}	1.25115^{4}	1.96261^{9}	1.66319^{8}	1.02113^{1}	1.04133^{2}
	MSE	$\hat{a}$	0.10536^{5}	0.12531^{7}	0.11095^{6}	0.08396^{3}	0.09299^{4}	0.14475^{9}	0.13324^{8}	0.04746^{2}	0.04382^{1}
		$\hat{b}$	8.37793^{5}	9.11725^{6}	71.40863^{9}	2.61268^{3}	3.48420^{4}	16.13409	11.31605	1.04271^{1}	1.08436^{2}
	MRE	$\hat{a}$	0.20129^{4}	0.22759^{8}	0.20652^{6}	0.19713^{3}	0.20478^{5}	0.23332^{9}	0.22758^{7}	0.18155^{2}	0.17445^{1}
		$\hat{b}$	0.45579^{5}	0.46928^{7}	0.46422^{6}	0.33374^{3}	0.35747^{4}	0.56074^{9}	0.47520^{8}	0.29175^{1}	0.29752^{2}
	$\sum$ Ranks		28^{5}	43^{7}	39^{6}	18^{3}	26^{4}	53^{9}	45^{8}	$9^{1.5}$	$9^{1.5}$
50	AB	$\hat{a}$	0.14568^{3}	0.16489^{8}	0.14850^{5}	0.14617^{4}	0.15174^{6}	0.16830^{9}	0.16360^{7}	0.13542^{2}	0.12838^{1}
		$\hat{b}$	0.80276^{5}	0.88653^{8}	0.81413^{6}	0.71308^{3}	0.74621^{4}	0.96930^{9}	0.87157^{7}	0.65070^{2}	0.64771^{1}
	MSE	$\hat{a}$	0.03513^{4}	0.04437^{8}	0.03567^{6}	0.03154^{3}	0.03531^{5}	0.04700^{9}	0.04397^{7}	0.01834^{2}	0.01648^{1}
		$\hat{b}$	1.26655^{5}	1.54885^{7}	1.29593^{6}	0.78762^{3}	0.92146^{4}	1.96423^{9}	1.55936^{8}	0.42341^{2}	0.41953^{1}
	MRE	$\hat{a}$	0.12140^{3}	0.13741^{8}	0.12375^{5}	0.12180^{4}	0.12645^{6}	0.14025^{9}	0.13633^{7}	0.11285^{2}	0.10698^{1}
		$\hat{b}$	0.22936^{5}	0.25329^{8}	0.23261^{6}	0.20374^{3}	0.21320^{4}	0.27694^{9}	0.24902^{7}	0.18591^{2}	0.18506^{1}
	$\sum$ Ranks		25^{4}	47^{8}	34^{6}	20^{3}	29^{5}	54^{9}	43^{7}	12^{2}	6^{1}
100	AB	$\hat{a}$	0.09714^{3}	0.11411^{7}	0.10292^{5}	0.10042^{4}	0.10643^{6}	0.11473^{8}	0.11749^{9}	0.09664^{2}	0.08971^{1}
		$\hat{b}$	0.52447^{4}	0.59169^{7}	0.54203^{6}	0.49126^{3}	0.52489^{5}	0.62384^{9}	0.59953^{8}	0.46784^{2}	0.45035^{1}
	MSE	$\hat{a}$	0.01513^{3}	0.02055^{7}	0.01713^{5}	0.01551^{4}	0.01756^{6}	0.02124^{8}	0.02255^{9}	0.00934^{2}	0.00805^{1}
		$\hat{b}$	0.47707^{5}	0.59926^{7}	0.51402^{6}	0.37864^{3}	0.45102^{4}	0.68860^{9}	0.65470^{8}	0.21887^{2}	0.20282^{1}
	MRE	$\hat{a}$	0.08095^{3}	0.09509^{7}	0.08576^{5}	0.08368^{4}	0.08869^{6}	0.09561^{8}	0.09791^{9}	0.08053^{2}	0.07476^{1}
		$\hat{b}$	0.14985^{4}	0.16905^{7}	0.15487^{6}	0.14036^{3}	0.14997^{5}	0.17824^{9}	0.17130^{8}	0.13367^{2}	0.12867^{1}
	$\sum$ Ranks		22^{4}	42^{7}	33^{6}	21^{3}	32^{5}	$51^{8.5}$	$51^{8.5}$	12^{2}	6^{1}
250	AB	$\hat{a}$	0.06096^{3}	0.07142^{7}	0.06586^{5}	0.06264^{4}	0.06594^{6}	0.07361^{9}	0.07274^{8}	0.06094^{2}	0.05604^{1}
		$\hat{b}$	0.31765^{4}	0.36972^{8}	0.34544^{6}	0.30280^{3}	0.32841^{5}	0.38769^{9}	0.36509^{7}	0.30140^{2}	0.28429^{1}
	MSE	$\hat{a}$	0.00596^{3}	0.00813^{7}	0.00688^{6}	0.00611^{4}	0.00680^{5}	0.00873^{9}	0.00844^{8}	0.00371^{2}	0.00314^{1}
		$\hat{b}$	0.16852^{4}	0.22438^{8}	0.19453^{6}	0.15335^{3}	0.17214^{5}	0.24924^{9}	0.22033^{7}	0.09084^{2}	0.08082^{1}
	MRE	$\hat{a}$	0.05080^{3}	0.05952^{7}	0.05488^{5}	0.05220^{4}	0.05495^{6}	0.06134^{9}	0.06062^{8}	0.05078^{2}	0.04670^{1}
		$\hat{b}$	0.09076^{4}	0.10563^{8}	0.09870^{6}	0.08651^{3}	0.09383^{5}	0.11077^{9}	0.10431^{7}	0.08611^{2}	0.08123^{1}
	$\sum$ Ranks		$21^{3.5}$	$45^{7.5}$	34^{6}	$21^{3.5}$	32^{5}	54^{9}	$45^{7.5}$	12^{2}	6^{1}

Table 7. Simulation results for the nine estimation methods for $a = 1.7$ and $b = 2.5$.

n	Est.	Par.	MLEs	LSEs	WLSEs	MPSEs	PCEs	CVMEs	ADEs	RTADEs	MMEs
20	AB	$\hat{a}$	0.36563^{5}	0.39788^{7}	0.37849^{6}	0.35631^{4}	0.33638^{3}	0.43469^{9}	0.42643^{8}	0.33572^{2}	0.28808^{1}
		$\hat{b}$	1.00223^{6}	1.03492^{7}	0.99117^{5}	0.77506^{4}	0.74190^{3}	1.25220^{9}	1.11428^{8}	0.70877^{2}	0.62783^{1}
	MSE	$\hat{a}$	0.24254^{5}	0.27810^{7}	0.25096^{6}	0.19000^{4}	0.17334^{3}	0.34672^{9}	0.33498^{8}	0.11271^{2}	0.08299^{1}
		$\hat{b}$	2.75565^{5}	4.60139^{8}	3.20674^{6}	1.27464^{4}	1.05565^{3}	5.46849^{9}	4.21730^{7}	0.50235^{2}	0.39417^{1}
	MRE	$\hat{a}$	0.21507^{5}	0.23405^{7}	0.22264^{6}	0.20959^{4}	0.19787^{3}	0.25570^{9}	0.25084^{8}	0.19748^{2}	0.16946^{1}
		$\hat{b}$	0.40089^{6}	0.41397^{7}	0.39647^{5}	0.31002^{4}	0.29676^{3}	0.50088^{9}	0.44571^{8}	0.28351^{2}	0.25113^{1}
	$\sum$ Ranks		32^{5}	43^{7}	34^{6}	24^{4}	18^{3}	54^{9}	47^{8}	12^{2}	6^{1}
50	AB	$\hat{a}$	0.21185^{3}	0.24207^{6}	0.22921^{5}	0.22323^{4}	0.20941^{2}	0.25299^{7}	0.25355^{8}	0.20499^{2}	0.17131^{1}
		$\hat{b}$	0.51360^{4}	0.56291^{6}	0.52964^{5}	0.47765^{3}	0.46302^{2}	0.61947^{8}	0.57508^{7}	0.43800^{2}	0.38089^{1}
	MSE	$\hat{a}$	0.07404^{3}	0.09601^{6}	0.08467^{5}	0.07516^{4}	0.06833^{2}	0.10855^{8}	0.10844^{7}	0.04202^{2}	0.02935^{1}
		$\hat{b}$	0.49756^{4}	0.61614^{6}	0.52115^{5}	0.36327^{3}	0.35283^{2}	0.78932^{8}	0.65699^{7}	0.19184^{2}	0.14507^{1}
	MRE	$\hat{a}$	0.12461^{3}	0.14239^{6}	0.13483^{5}	0.13131^{4}	0.12318^{2}	0.14882^{7}	0.14915^{8}	0.12058^{2}	0.10077^{1}
		$\hat{b}$	0.20544^{4}	0.22516^{6}	0.21186^{5}	0.19106^{3}	0.18521^{2}	0.24779^{8}	0.23003^{7}	0.17520^{2}	0.15235^{1}
	$\sum$ Ranks		$21^{4.5}$	36^{7}	30^{6}	$21^{4.5}$	$12^{2.5}$	46^{9}	44^{8}	$12^{2.5}$	6^{1}
100	AB	$\hat{a}$	0.14921^{4}	0.17071^{7}	0.15732^{6}	0.15146^{5}	0.14692^{3}	0.17779^{9}	0.17727^{8}	0.14636^{2}	0.12348^{1}
		$\hat{b}$	0.34599^{5}	0.38709^{7}	0.36181^{6}	0.32779^{4}	0.32726^{3}	0.41573^{9}	0.38732^{8}	0.30836^{2}	0.27591^{1}
	MSE	$\hat{a}$	0.03586^{5}	0.04701^{7}	0.03955^{6}	0.03467^{4}	0.03368^{3}	0.05161^{9}	0.05099^{8}	0.02142^{2}	0.01525^{1}
		$\hat{b}$	0.20609^{5}	0.25804^{7}	0.22678^{6}	0.16485^{3}	0.16989^{4}	0.31503^{9}	0.26518^{8}	0.09508^{2}	0.07613^{1}
	MRE	$\hat{a}$	0.08777^{4}	0.10042^{7}	0.09254^{6}	0.08910^{5}	0.08643^{3}	0.10458^{9}	0.10428^{8}	0.08609^{2}	0.07263^{1}
		$\hat{b}$	0.13840^{5}	0.15484^{7}	0.14473^{6}	0.13112^{4}	0.13090^{3}	0.16629^{9}	0.15493^{8}	0.12334^{2}	0.11036^{1}
	$\sum$ Ranks		28^{5}	42^{7}	36^{6}	25^{4}	19^{3}	54^{9}	48^{8}	12^{2}	6^{1}
250	AB	$\hat{a}$	0.09282^{4}	0.10986^{8}	0.09704^{6}	0.09573^{5}	0.09279^{3}	0.10844^{7}	0.11085^{9}	0.09266^{2}	0.07980^{1}
		$\hat{b}$	0.21078^{5}	0.24773^{9}	0.21695^{6}	0.20645^{4}	0.20345^{3}	0.24767^{8}	0.24067^{7}	0.19412^{2}	0.17655^{1}
	MSE	$\hat{a}$	0.01364^{4}	0.01910^{8}	0.01472^{6}	0.01429^{5}	0.01357^{3}	0.01896^{7}	0.01948^{9}	0.00859^{2}	0.00637^{1}
		$\hat{b}$	0.07252^{5}	0.09991^{8}	0.07571^{6}	0.06756^{4}	0.06646^{3}	0.10108^{9}	0.09476^{7}	0.03768^{2}	0.03117^{1}
	MRE	$\hat{a}$	0.05460^{4}	0.06462^{8}	0.05708^{6}	0.05631^{5}	0.05458^{3}	0.06379^{7}	0.06521^{9}	0.05450^{2}	0.04694^{1}
		$\hat{b}$	0.08431^{5}	0.09909^{9}	0.08678^{6}	0.08258^{4}	0.08138^{3}	0.09907^{8}	0.09627^{7}	0.07765^{2}	0.07062^{1}
	$\sum$ Ranks		$27^{4.5}$	50^{9}	36^{6}	$27^{4.5}$	18^{3}	46^{7}	48^{8}	12^{2}	6^{1}

Table 8. Simulation results for the nine estimation methods for $a = 2.3$ and $b = 2$.

n	Est.	Par.	MLEs	LSEs	WLSEs	MPSEs	PCEs	CVMEs	ADEs	RTADEs	MMEs
20	AB	$\hat{a}$	0.52023^{5}	0.56468^{7}	0.53722^{6}	0.50405^{4}	0.48991^{3}	0.63080^{9}	0.60674^{8}	0.46959^{2}	0.41088^{1}
		$\hat{b}$	0.74232^{6}	0.76585^{7}	0.73575^{5}	0.58650^{3}	0.59552^{4}	0.96590^{9}	0.80481^{8}	0.52968^{2}	0.48818^{1}
	MSE	$\hat{a}$	0.49382^{5}	0.56378^{7}	0.50903^{6}	0.38024^{4}	0.36491^{3}	0.74537^{9}	0.68060^{8}	0.22052^{2}	0.16883^{1}
		$\hat{b}$	1.43191^{5}	2.06908^{7}	1.60023^{6}	0.68784^{4}	0.67717^{3}	4.46991^{9}	2.15837^{8}	0.28056^{2}	0.23832^{1}
	MRE	$\hat{a}$	0.22618^{5}	0.24551^{7}	0.23358^{6}	0.21915^{4}	0.21300^{3}	0.27426^{9}	0.26380^{8}	0.20417^{2}	0.17865^{1}
		$\hat{b}$	0.37116^{6}	0.38293^{7}	0.36787^{5}	0.29325^{3}	0.29776^{4}	0.48295^{9}	0.40241^{8}	0.26484^{2}	0.24409^{1}
	$\sum$ Ranks		32^{5}	42^{7}	34^{6}	22^{4}	20^{3}	54^{9}	48^{8}	12^{2}	6^{1}
50	AB	$\hat{a}$	0.30093^{4}	0.34348^{7}	0.32539^{6}	0.31619^{5}	0.29988^{3}	0.36330^{9}	0.35740^{8}	0.29580^{2}	0.24870^{1}
		$\hat{b}$	0.38674^{5}	0.42322^{7}	0.39848^{6}	0.36243^{4}	0.34981^{3}	0.46749^{9}	0.42501^{8}	0.32793^{2}	0.30095^{1}
	MSE	$\hat{a}$	0.14984^{4}	0.19373^{7}	0.17102^{6}	0.15070^{5}	0.13897^{3}	0.22189^{9}	0.21431^{8}	0.08750^{2}	0.06185^{1}
		$\hat{b}$	0.27830^{5}	0.33989^{7}	0.28931^{6}	0.20710^{4}	0.20221^{3}	0.42154^{9}	0.35481^{8}	0.10754^{2}	0.09057^{1}
	MRE	$\hat{a}$	0.13084^{4}	0.14934^{7}	0.14148^{6}	0.13747^{5}	0.13038^{3}	0.15795^{9}	0.15539^{8}	0.12861^{2}	0.10813^{1}
		$\hat{b}$	0.19337^{5}	0.21161^{7}	0.19924^{6}	0.18122^{4}	0.17490^{3}	0.23374^{9}	0.21250^{8}	0.16397^{2}	0.15048^{1}
	$\sum$ Ranks		$27^{4.5}$	42^{7}	36^{6}	$27^{4.5}$	18^{3}	54^{9}	48^{8}	12^{2}	6^{1}
100	AB	$\hat{a}$	0.21188^{4}	0.24227^{7}	0.22331^{6}	0.21481^{5}	0.20925^{3}	0.24904^{8}	0.25197^{9}	0.20787^{2}	0.17962^{1}
		$\hat{b}$	0.26142^{5}	0.29192^{7}	0.27325^{6}	0.24980^{4}	0.24965^{3}	0.30837^{9}	0.29463^{8}	0.23354^{2}	0.21387^{1}
	MSE	$\hat{a}$	0.07242^{5}	0.09478^{7}	0.07978^{6}	0.06967^{4}	0.06743^{3}	0.09995^{8}	0.10194^{9}	0.04321^{2}	0.03226^{1}
		$\hat{b}$	0.11676^{5}	0.14533^{7}	0.12819^{6}	0.09514^{3}	0.09839^{4}	0.16725^{9}	0.15148^{8}	0.05454^{2}	0.04574^{1}
	MRE	$\hat{a}$	0.09212^{4}	0.10533^{7}	0.09709^{6}	0.09340^{5}	0.09098^{3}	0.10828^{8}	0.10955^{9}	0.09038^{2}	0.07810^{1}
		$\hat{b}$	0.13071^{5}	0.14596^{7}	0.13662^{6}	0.12490^{4}	0.12483^{3}	0.15418^{9}	0.14731^{8}	0.11677^{2}	0.10694^{1}
	$\sum$ Ranks		28^{5}	42^{7}	36^{6}	25^{4}	19^{3}	$51^{8.5}$	$51^{8.5}$	12^{2}	6^{1}
250	AB	$\hat{a}$	0.13185^{2}	0.15586^{9}	0.13770^{6}	0.13592^{5}	0.13346^{3}	0.15445^{7}	0.15513^{8}	0.13506^{4}	0.11178^{1}
		$\hat{b}$	0.15972^{4}	0.18724^{9}	0.16412^{6}	0.15850^{3}	0.16032^{5}	0.18517^{8}	0.17835^{7}	0.15097^{2}	0.13575^{1}
	MSE	$\hat{a}$	0.02753^{3}	0.03845^{7}	0.02966^{6}	0.02881^{5}	0.02777^{4}	0.03887^{9}	0.03855^{8}	0.01824^{2}	0.01249^{1}
		$\hat{b}$	0.04148^{5}	0.05683^{8}	0.04322^{6}	0.03904^{3}	0.04019^{4}	0.05763^{9}	0.05209^{7}	0.02279^{2}	0.01843^{1}
	MRE	$\hat{a}$	0.05733^{2}	0.06777^{9}	0.05987^{6}	0.05909^{5}	0.05802^{3}	0.06715^{7}	0.06745^{8}	0.05872^{4}	0.04860^{1}
		$\hat{b}$	0.07986^{4}	0.09362^{9}	0.08206^{6}	0.07925^{3}	0.08016^{5}	0.09259^{8}	0.08917^{7}	0.07548^{2}	0.06787^{1}
	$\sum$ Ranks		20^{3}	51^{9}	36^{6}	$24^{4.5}$	$24^{4.5}$	48^{8}	45^{7}	16^{2}	6^{1}

Table 9. Simulation results for the nine estimation methods for $a = 1.3$ and $b = 0.5$.

n	Est.	Par.	MLEs	LSEs	WLSEs	MPSEs	PCEs	CVMEs	ADEs	RTADEs	MMEs
20	AB	$\hat{a}$	0.48498^{4}	0.53597^{7}	0.48723^{5}	0.41671^{2}	0.49731^{6}	0.60604^{8}	0.65002^{9}	0.45233^{3}	0.03152^{1}
		$\hat{b}$	0.11919^{5}	0.13067^{6}	0.11834^{4}	0.10124^{3}	0.13482^{7}	0.14734^{9}	0.13931^{8}	0.10054^{2}	0.08322^{1}
	MSE	$\hat{a}$	0.48217^{5}	0.58823^{7}	0.48390^{6}	0.27942^{3}	0.41164^{4}	0.87348^{8}	1.00429^{9}	0.20460^{2}	0.00099^{1}
		$\hat{b}$	0.02889^{4}	0.03886^{7}	0.03232^{6}	0.01649^{3}	0.03106^{5}	0.06573^{9}	0.04414^{8}	0.01011^{2}	0.00693^{1}
	MRE	$\hat{a}$	0.37306^{4}	0.41229^{7}	0.37479^{5}	0.32055^{2}	0.38254^{6}	0.46618^{8}	0.50002^{9}	0.34795^{3}	0.02425^{1}
		$\hat{b}$	0.23838^{5}	0.26134^{6}	0.23667^{4}	0.20247^{3}	0.26963^{7}	0.29467^{9}	0.27861^{8}	0.20109^{2}	0.16644^{1}
	$\sum$ Ranks		27^{4}	40^{7}	30^{5}	16^{3}	35^{6}	$51^{8.5}$	$51^{8.5}$	14^{2}	6^{1}
50	AB	$\hat{a}$	0.26989^{3}	0.31300^{6}	0.30230^{5}	0.25838^{2}	0.31389^{7}	0.33169^{8}	0.36241^{9}	0.27883^{4}	0.02335^{1}
		$\hat{b}$	0.06700^{4}	0.07439^{6}	0.07306^{5}	0.06223^{2}	0.08456^{9}	0.07945^{8}	0.07821^{7}	0.06226^{3}	0.05791^{1}
	MSE	$\hat{a}$	0.13392^{4}	0.16624^{7}	0.15877^{6}	0.10443^{3}	0.15077^{5}	0.19827^{8}	0.24159^{9}	0.07774^{2}	0.00055^{1}
		$\hat{b}$	0.00803^{4}	0.00940^{6}	0.00929^{5}	0.00616^{3}	0.01138^{9}	0.01131^{8}	0.01071^{7}	0.00388^{2}	0.00335^{1}
	MRE	$\hat{a}$	0.20761^{3}	0.24077^{6}	0.23254^{5}	0.19876^{2}	0.24145^{7}	0.25514^{8}	0.27878^{9}	0.21448^{4}	0.01796^{1}
		$\hat{b}$	0.13400^{4}	0.14877^{6}	0.14612^{5}	0.12447^{2}	0.16913^{9}	0.15890^{8}	0.15642^{7}	0.12451^{3}	0.11581^{1}
	$\sum$ Ranks		22^{4}	37^{6}	31^{5}	14^{2}	46^{7}	$48^{8.5}$	$48^{8.5}$	18^{3}	6^{1}
100	AB	$\hat{a}$	0.17973^{3}	0.22723^{7}	0.20263^{5}	0.17331^{2}	0.21877^{6}	0.23347^{8}	0.24357^{9}	0.19952^{4}	0.01788^{1}
		$\hat{b}$	0.04324^{3}	0.05281^{6}	0.04905^{5}	0.04234^{2}	0.05895^{9}	0.05480^{8}	0.05292^{7}	0.04450^{4}	0.04009^{1}
	MSE	$\hat{a}$	0.05770^{4}	0.08393^{7}	0.06770^{5}	0.04971^{3}	0.07350^{6}	0.09043^{8}	0.10162^{9}	0.03981^{2}	0.00032^{1}
		$\hat{b}$	0.00333^{4}	0.00456^{6}	0.00392^{5}	0.00297^{3}	0.00547^{9}	0.00492^{8}	0.00470^{7}	0.00198^{2}	0.00161^{1}
	MRE	$\hat{a}$	0.13825^{3}	0.17479^{7}	0.15587^{5}	0.13332^{2}	0.16828^{6}	0.17960^{8}	0.18736^{9}	0.15348^{4}	0.01376^{1}
		$\hat{b}$	0.08649^{3}	0.10562^{6}	0.09811^{5}	0.08469^{2}	0.11790^{9}	0.10960^{8}	0.10583^{7}	0.08899^{4}	0.08018^{1}
	$\sum$ Ranks		$20^{3.5}$	39^{6}	30^{5}	14^{2}	45^{7}	$48^{8.5}$	$48^{8.5}$	$20^{3.5}$	6^{1}
250	AB	$\hat{a}$	0.09900^{2}	0.13890^{6}	0.12580^{5}	0.09994^{3}	0.13960^{7}	0.14602^{8}	0.15210^{9}	0.12269^{4}	0.00938^{1}
		$\hat{b}$	0.02477^{2}	0.03313^{7}	0.03041^{5}	0.02438^{1}	0.03811^{9}	0.03402^{8}	0.03305^{6}	0.02792^{4}	0.02560^{3}
	MSE	$\hat{a}$	0.01926^{4}	0.03093^{7}	0.02509^{5}	0.01838^{3}	0.03007^{6}	0.03407^{8}	0.03747^{9}	0.01505^{2}	0.00009^{1}
		$\hat{b}$	0.00119^{4}	0.00175^{6}	0.00148^{5}	0.00111^{3}	0.00224^{9}	0.00185^{8}	0.00176^{7}	0.00078^{2}	0.00066^{1}
	MRE	$\hat{a}$	0.07616^{2}	0.10684^{6}	0.09677^{5}	0.07688^{3}	0.10738^{7}	0.11232^{8}	0.11700^{9}	0.09438^{4}	0.00722^{1}
		$\hat{b}$	0.04954^{2}	0.06626^{7}	0.06083^{5}	0.04876^{1}	0.07622^{9}	0.06804^{8}	0.06611^{6}	0.05584^{4}	0.05120^{3}
	$\sum$ Ranks		16^{3}	39^{6}	30^{5}	14^{2}	47^{8}	48^{9}	46^{7}	20^{4}	10^{1}

Table 10. Simulation results for the nine estimation methods for $a = 2.5$ and $b = 2.5$.

n	Est.	Par.	MLEs	LSEs	WLSEs	MPSEs	PCEs	CVMEs	ADEs	RTADEs	MMEs
20	AB	$\hat{a}$	0.53981^{5}	0.60511^{7}	0.56260^{6}	0.51774^{4}	0.50642^{3}	0.65046^{9}	0.61146^{8}	0.49472^{2}	0.43730^{1}
		$\hat{b}$	1.00834^{6}	1.11449^{8}	0.96928^{5}	0.74894^{3}	0.76762^{4}	1.32945^{9}	1.07159^{7}	0.70526^{2}	0.64903^{1}
	MSE	$\hat{a}$	0.52189^{5}	0.65095^{7}	0.54703^{6}	0.40517^{4}	0.39638^{3}	0.82038^{9}	0.70769^{8}	0.24475^{2}	0.19123^{1}
		$\hat{b}$	2.75079^{5}	6.39134^{8}	3.30852^{6}	0.99852^{3}	1.19467^{4}	8.17979^{9}	4.12461^{7}	0.49739^{2}	0.42124^{1}
	MRE	$\hat{a}$	0.21592^{5}	0.24205^{7}	0.22504^{6}	0.20710^{4}	0.20257^{3}	0.26018^{9}	0.24458^{8}	0.19789^{2}	0.17492^{1}
		$\hat{b}$	0.40334^{6}	0.44580^{8}	0.38771^{5}	0.29958^{3}	0.30705^{4}	0.53178^{9}	0.42864^{7}	0.28210^{2}	0.25961^{1}
	$\sum$ Ranks		32^{5}	$45^{7.5}$	34^{6}	$21^{3.5}$	$21^{3.5}$	54^{9}	$45^{7.5}$	12^{2}	6^{1}
50	AB	$\hat{a}$	0.31599^{4}	0.35948^{7}	0.33657^{6}	0.32260^{5}	0.31464^{3}	0.38422^{9}	0.36967^{8}	0.29839^{2}	0.26121^{1}
		$\hat{b}$	0.51766^{5}	0.57047^{8}	0.53624^{6}	0.47233^{4}	0.46852^{3}	0.63817^{9}	0.56953^{7}	0.42878^{2}	0.40074^{1}
	MSE	$\hat{a}$	0.16777^{5}	0.21183^{7}	0.17891^{6}	0.15796^{4}	0.15308^{3}	0.24673^{9}	0.22999^{8}	0.08903^{2}	0.06823^{1}
		$\hat{b}$	0.51315^{5}	0.63971^{7}	0.53174^{6}	0.34703^{3}	0.36202^{4}	0.83900^{9}	0.65368^{8}	0.18386^{2}	0.16059^{1}
	MRE	$\hat{a}$	0.12640^{4}	0.14379^{7}	0.13463^{6}	0.12904^{5}	0.12585^{3}	0.15369^{9}	0.14787^{8}	0.11935^{2}	0.10448^{1}
		$\hat{b}$	0.20706^{5}	0.22819^{8}	0.21450^{6}	0.18893^{4}	0.18741^{3}	0.25527^{9}	0.22781^{7}	0.17151^{2}	0.16030^{1}
	$\sum$ Ranks		28^{5}	44^{7}	36^{6}	25^{4}	19^{3}	54^{9}	46^{8}	12^{2}	6^{1}
100	AB	$\hat{a}$	0.21648^{3}	0.25459^{7}	0.23447^{6}	0.22676^{5}	0.22030^{4}	0.25875^{9}	0.25774^{8}	0.20790^{2}	0.17989^{1}
		$\hat{b}$	0.34136^{5}	0.39588^{8}	0.36696^{6}	0.33589^{4}	0.32795^{3}	0.41001^{9}	0.38788^{7}	0.30246^{2}	0.27461^{1}
	MSE	$\hat{a}$	0.07654^{4}	0.10249^{7}	0.08743^{6}	0.07934^{5}	0.07454^{3}	0.10947^{9}	0.10780^{8}	0.04322^{2}	0.03236^{1}
		$\hat{b}$	0.19815^{5}	0.26186^{7}	0.23096^{6}	0.17461^{4}	0.17092^{3}	0.29815^{9}	0.26680^{8}	0.09148^{2}	0.07541^{1}
	MRE	$\hat{a}$	0.08659^{3}	0.10184^{7}	0.09379^{6}	0.09070^{5}	0.08812^{4}	0.10350^{9}	0.10309^{8}	0.08316^{2}	0.07196^{1}
		$\hat{b}$	0.13655^{5}	0.15835^{8}	0.14678^{6}	0.13436^{4}	0.13118^{3}	0.16400^{9}	0.15515^{7}	0.12098^{2}	0.10984^{1}
	$\sum$ Ranks		25^{4}	44^{7}	36^{6}	27^{5}	20^{3}	54^{9}	46^{8}	12^{2}	6^{1}
250	AB	$\hat{a}$	0.13774^{4}	0.16317^{9}	0.14344^{6}	0.13851^{5}	0.13769^{3}	0.16231^{7}	0.16263^{8}	0.13353^{2}	0.11175^{1}
		$\hat{b}$	0.21158^{5}	0.24961^{8}	0.21944^{6}	0.20723^{3}	0.20976^{4}	0.25230^{9}	0.23924^{7}	0.19493^{2}	0.17041^{1}
	MSE	$\hat{a}$	0.03023^{5}	0.04174^{7}	0.03283^{6}	0.02927^{3}	0.02975^{4}	$0.04181^{8.}$	$0.04181^{8.}$	0.01783^{2}	0.01249^{1}
		$\hat{b}$	0.07329^{5}	0.10088^{8}	0.07859^{6}	0.06591^{3}	0.06862^{4}	0.10619^{9}	0.09284^{7}	0.03800^{2}	0.02904^{1}
	MRE	$\hat{a}$	0.05509^{4}	0.06527^{9}	0.05737^{6}	0.05541^{5}	0.05507^{3}	0.06492^{7}	0.06505^{8}	0.05341^{2}	0.04470^{1}
		$\hat{b}$	0.08463^{5}	0.09984^{8}	0.08778^{6}	0.08289^{3}	0.08391^{4}	0.10092^{9}	0.09570^{7}	0.07797^{2}	0.06817^{1}
	$\sum$ Ranks		28^{5}	49^{8}	36^{6}	$22^{3.5}$	$22^{3.5}$	49.5^{9}	45.5^{7}	12^{2}	6^{1}

Table 11. Simulation results for the nine estimation methods for $a = 3.5$ and $b = 0.7$.

n	Est.	Par.	MLEs	LSEs	WLSEs	MPSEs	PCEs	CVMEs	ADEs	RTADEs	MMEs
20	AB	$\hat{a}$	1.13977^{5}	1.20546^{8}	1.14879^{6}	1.03098^{2}	1.19426^{7}	1.38979^{9}	1.06029^{4}	1.03344^{3}	0.59919^{1}
		$\hat{b}$	0.18651^{6}	0.19025^{7}	0.18296^{5}	0.15923^{3}	0.19794^{8}	0.23250^{9}	0.17158^{4}	0.14801^{1}	0.15535^{2}
	MSE	$\hat{a}$	2.53713^{7}	2.62581^{8}	2.41989^{6}	1.63769^{3}	2.28491^{5}	4.03467^{9}	2.03020^{4}	1.06799^{2}	0.35903^{1}
		$\hat{b}$	0.07440^{7}	0.07892^{8}	0.07418^{6}	0.04188^{3}	0.06720^{5}	0.13148^{9}	0.05907^{4}	0.02191^{1}	0.02413^{2}
	MRE	$\hat{a}$	0.32565^{5}	0.34442^{8}	0.32823^{6}	0.29457^{2}	0.34122^{7}	0.39708^{9}	0.30294^{4}	0.29527^{3}	0.17120^{1}
		$\hat{b}$	0.26644^{6}	0.27179^{7}	0.26137^{5}	0.22747^{3}	0.28277^{8}	0.33214^{9}	0.24511^{4}	0.21144^{1}	0.22193^{2}
	$\sum$ Ranks		36^{6}	46^{8}	34^{5}	16^{3}	40^{7}	54^{9}	24^{4}	11^{2}	9^{1}
50	AB	$\hat{a}$	0.64358^{4}	0.74995^{7}	0.68887^{6}	0.62929^{2}	0.75209^{8}	0.76531^{9}	0.65055^{5}	0.63909^{3}	0.43708^{1}
		$\hat{b}$	0.10452^{5}	0.11654^{7}	0.10878^{6}	0.09907^{3}	0.12714^{9}	0.12258^{8}	0.10335^{4}	0.09363^{2}	0.09038^{1}
	MSE	$\hat{a}$	0.69667^{4}	0.93765^{8}	0.79634^{6}	0.60295^{3}	0.87168^{7}	1.04823^{9}	0.72716^{5}	0.40844^{2}	0.19104^{1}
		$\hat{b}$	0.01923^{5}	0.02354^{7}	0.02032^{6}	0.01498^{3}	0.02554^{8}	0.02813^{9}	0.01865^{4}	0.00877^{2}	0.00817^{1}
	MRE	$\hat{a}$	0.18388^{4}	0.21427^{7}	0.19682^{6}	0.17980^{2}	0.21488^{8}	0.21866^{9}	0.18587^{5}	0.18260^{3}	0.12488^{1}
		$\hat{b}$	0.14931^{5}	0.16648^{7}	0.15540^{6}	0.14153^{3}	0.18163^{9}	0.17512^{8}	0.14765^{4}	0.13376^{2}	0.12912^{1}
	$\sum$ Ranks		$27^{4.5}$	43^{7}	36^{6}	16^{3}	49^{8}	52^{9}	$27^{4.5}$	14^{2}	6^{1}
100	AB	$\hat{a}$	0.44682^{3}	0.51166^{7}	0.46691^{6}	0.43625^{2}	0.54676^{9}	0.53150^{8}	0.46085^{4}	0.46112^{5}	0.28787^{1}
		$\hat{b}$	0.07187^{4}	0.07941^{7}	0.07403^{6}	0.06728^{3}	0.09353^{9}	0.08457^{8}	0.07247^{5}	0.06643^{2}	0.05365^{1}
	MSE	$\hat{a}$	0.32581^{4}	0.42404^{7}	0.35235^{6}	0.29694^{3}	0.45283^{8}	0.46315^{9}	0.34666^{5}	0.21263^{2}	0.08287^{1}
		$\hat{b}$	0.00858^{4}	0.01062^{7}	0.00905^{6}	0.00708^{3}	0.01358^{9}	0.01241^{8}	0.00876^{5}	0.00441^{2}	0.00288^{1}
	MRE	$\hat{a}$	0.12766^{3}	0.14619^{7}	0.13340^{6}	0.12464^{2}	0.15622^{9}	0.15186^{8}	0.13167^{4}	0.13175^{5}	0.08225^{1}
		$\hat{b}$	0.10267^{4}	0.11345^{7}	0.10576^{6}	0.09612^{3}	0.13361^{9}	0.12082^{8}	0.10353^{5}	0.09490^{2}	0.07664^{1}
	$\sum$ Ranks		22^{4}	42^{7}	36^{6}	16^{2}	53^{9}	49^{8}	28^{5}	18^{3}	6^{1}
250	AB	$\hat{a}$	0.26882^{3}	0.32188^{7}	0.29088^{6}	0.26250^{2}	0.34968^{9}	0.32698^{8}	0.28105^{4}	0.28463^{5}	0.13342^{1}
		$\hat{b}$	0.04302^{4}	0.04963^{7}	0.04598^{6}	0.04241^{3}	0.06036^{9}	0.05030^{8}	0.04407^{5}	0.04129^{2}	0.03716^{1}
	MSE	$\hat{a}$	0.11693^{4}	0.16443^{7}	0.13531^{6}	0.11490^{3}	0.18875^{9}	0.17142^{8}	0.12779^{5}	0.08102^{2}	0.01780^{1}
		$\hat{b}$	0.00307^{4}	0.00395^{7}	0.00339^{6}	0.00284^{3}	0.00566^{9}	0.00412^{8}	0.00316^{5}	0.00170^{2}	0.00138^{1}
	MRE	$\hat{a}$	0.07681^{3}	0.09197^{7}	0.08311^{6}	0.07500^{2}	0.09991^{9}	0.09342^{8}	0.08030^{4}	0.08132^{5}	0.03812^{1}
		$\hat{b}$	0.06145^{4}	0.07090^{7}	0.06569^{6}	0.06058^{3}	0.08623^{9}	0.07186^{8}	0.06296^{5}	0.05899^{2}	0.05309^{1}
	$\sum$ Ranks		22^{4}	42^{7}	36^{6}	16^{2}	54^{9}	48^{8}	28^{5}	18^{3}	6^{1}

Table 12. Simulation results for the nine estimation methods for $a = 0.4$ and $b = 1.25$.

n	Est.	Par.	MLEs	LSEs	WLSEs	MPSEs	PCEs	CVMEs	ADEs	RTADEs	MMEs
20	AB	$\hat{a}$	0.10414^{4}	0.11515^{7}	0.10504^{5}	0.09819^{2}	0.13059^{9}	0.12780^{8}	0.10078^{3}	0.09429^{1}	0.10525^{6}
		$\hat{b}$	0.40030^{7}	0.42765^{8}	0.38286^{5}	0.32186^{3}	0.38974^{6}	0.50956^{9}	0.36179^{4}	0.29902^{1}	0.31366^{2}
	MSE	$\hat{a}$	0.02021^{6}	0.02348^{7}	0.01892^{5}	0.01444^{3}	0.02698^{8}	0.03165^{9}	0.01789^{4}	0.00889^{1}	0.01108^{2}
		$\hat{b}$	0.37856^{6}	0.55607^{8}	0.40053^{7}	0.17984^{3}	0.30048^{5}	0.81810^{9}	0.28872^{4}	0.08941^{1}	0.09838^{2}
	MRE	$\hat{a}$	0.26034^{4}	0.28788^{7}	0.26261^{5}	0.24548^{2}	0.32648^{9}	0.31950^{8}	0.25194^{3}	0.23572^{1}	0.26313^{6}
		$\hat{b}$	0.32024^{7}	0.34212^{8}	0.30628^{5}	0.25749^{3}	0.31179^{6}	0.40765^{9}	0.28943^{4}	0.23922^{1}	0.25092^{2}
	$\sum$ Ranks		34^{6}	45^{8}	32^{5}	16^{2}	43^{7}	52^{9}	22^{4}	6^{1}	20^{3}
50	AB	$\hat{a}$	0.05865^{1}	0.06898^{7}	0.06287^{5}	0.06029^{3}	0.08409^{9}	0.07189^{8}	0.06136^{4}	0.05870^{2}	0.06541^{6}
		$\hat{b}$	0.21162^{4}	0.24207^{7}	0.21599^{6}	0.19998^{3}	0.24890^{8}	0.25379^{9}	0.21473^{5}	0.18427^{1}	0.19753^{2}
	MSE	$\hat{a}$	0.00582^{4}	0.00761^{7}	0.00649^{6}	0.00546^{3}	0.01111^{9}	0.00889^{8}	0.00620^{5}	0.00345^{1}	0.00428^{2}
		$\hat{b}$	0.08164^{4}	0.10300^{7}	0.08241^{6}	0.06125^{3}	0.10761^{8}	0.12711^{9}	0.08215^{5}	0.03396^{1}	0.03902^{2}
	MRE	$\hat{a}$	0.14664^{1}	0.17245^{7}	0.15718^{5}	0.15073^{3}	0.21023^{9}	0.17972^{8}	0.15340^{4}	0.14674^{2}	0.16352^{6}
		$\hat{b}$	0.16930^{4}	0.19366^{7}	0.17279^{6}	0.15999^{3}	0.19912^{8}	0.20303^{9}	0.17178^{5}	0.14742^{1}	0.15802^{2}
	$\sum$ Ranks		$18^{2.5}$	42^{7}	34^{6}	$18^{2.5}$	$51^{8.5}$	$51^{8.5}$	28^{5}	8^{1}	20^{4}
100	AB	$\hat{a}$	0.04084^{1}	0.04851^{7}	0.04409^{5}	0.04109^{2}	0.05926^{9}	0.04946^{8}	0.04268^{4}	0.04157^{3}	0.04682^{6}
		$\hat{b}$	0.14347^{4}	0.16581^{7}	0.15362^{6}	0.13966^{2}	0.17525^{9}	0.17000^{8}	0.14726^{5}	0.13350^{1}	0.14306^{3}
	MSE	$\hat{a}$	0.00266^{4}	0.00381^{7}	0.00310^{6}	0.00257^{3}	0.00553^{8}	0.00400^{9}	0.00294^{5}	0.00173^{1}	0.00219^{2}
		$\hat{b}$	0.03450^{4}	0.04643^{7}	0.03970^{6}	0.03010^{3}	0.05017^{9}	0.04983^{8}	0.03611^{5}	0.01782^{1}	0.02047^{2}
	MRE	$\hat{a}$	0.10209^{1}	0.12127^{7}	0.11023^{5}	0.10274^{2}	0.14815^{9}	0.12364^{8}	0.10670^{4}	0.10391^{3}	0.11704^{6}
		$\hat{b}$	0.11478^{4}	0.13265^{7}	0.12289^{6}	0.11172^{2}	0.14020^{9}	0.13600^{8}	0.11781^{5}	0.10680^{1}	0.11445^{3}
	$\sum$ Ranks		18^{3}	42^{7}	34^{6}	14^{2}	53^{9}	49^{8}	28^{5}	10^{1}	22^{4}
250	AB	$\hat{a}$	0.02517^{1}	0.03048^{8}	0.02767^{5}	0.02595^{2}	0.03828^{9}	0.03039^{7}	0.02632^{4}	0.02615^{3}	0.02818^{6}
		$\hat{b}$	0.08672^{2}	0.10480^{8}	0.09366^{6}	0.08792^{3}	0.11224^{9}	0.10356^{7}	0.09061^{5}	0.08336^{1}	0.08811^{4}
	MSE	$\hat{a}$	0.00101^{3}	$0.00148^{7.5}$	0.00121^{6}	0.00105^{4}	0.00226^{9}	$0.00148^{7.5}$	0.00111^{5}	0.00068^{1}	0.00079^{2}
		$\hat{b}$	0.01222^{4}	0.01760^{7}	0.01419^{6}	0.01203^{3}	0.02006^{9}	0.01776^{8}	0.01331^{5}	0.00695^{1}	0.00776^{2}
	MRE	$\hat{a}$	0.06294^{1}	0.07620^{8}	0.06916^{5}	0.06489^{2}	0.09570^{9}	0.07599^{7}	0.06580^{4}	0.06537^{3}	0.07045^{6}
		$\hat{b}$	0.06938^{2}	0.08384^{8}	0.07493^{6}	0.07033^{3}	0.08979^{9}	0.08285^{7}	0.07249^{5}	0.06669^{1}	0.07049^{4}
	$\sum$ Ranks		13^{2}	46.5^{8}	34^{6}	17^{3}	54^{9}	43.5^{7}	28^{5}	10^{1}	24^{4}

Table 13. Simulation results for the nine estimation methods for $a = 0.7$ and $b = 0.9$.

n	Est.	Par.	MLEs	LSEs	WLSEs	MPSEs	PCEs	CVMEs	ADEs	RTADEs	MMEs
20	AB	$\hat{a}$	0.20556^{6}	0.21520^{8}	0.20792^{7}	0.18789^{3}	0.18977^{4}	0.24679^{9}	0.19117^{5}	0.18255^{2}	0.15910^{1}
		$\hat{b}$	0.26225^{8}	0.26102^{7}	0.25439^{6}	0.21520^{3}	0.22574^{4}	0.32220^{9}	0.23781^{5}	0.19742^{2}	0.18502^{1}
	MSE	$\hat{a}$	0.07895^{6}	0.08350^{8}	0.08060^{7}	0.05341^{3}	0.05823^{4}	0.12468^{9}	0.06563^{5}	0.03332^{2}	0.02531^{1}
		$\hat{b}$	0.14554^{6}	0.15374^{7}	0.16628^{8}	0.07577^{3}	0.08887^{4}	0.27233^{9}	0.11806^{5}	0.03898^{2}	0.03423^{1}
	MRE	$\hat{a}$	0.29366^{6}	0.30743^{8}	0.29703^{7}	0.26842^{3}	0.27110^{4}	0.35255^{9}	0.27311^{5}	0.26078^{2}	0.22729^{1}
		$\hat{b}$	0.29139^{8}	0.29002^{7}	0.28266^{6}	0.23912^{3}	0.25082^{4}	0.35799^{9}	0.26423^{5}	0.21936^{2}	0.20557^{1}
	$\sum$ Ranks		40^{6}	45^{8}	41^{7}	18^{3}	24^{4}	54^{9}	30^{5}	12^{2}	6^{1}
50	AB	$\hat{a}$	0.11390^{2}	0.13097^{8}	0.12360^{7}	0.11795^{4}	0.12064^{6}	0.14116^{9}	0.12034^{5}	0.11642^{3}	0.09966^{1}
		$\hat{b}$	0.13981^{4}	0.15326^{8}	0.14496^{7}	0.13445^{3}	0.14082^{5}	0.16855^{9}	0.14449^{6}	0.12892^{2}	0.11632^{1}
	MSE	$\hat{a}$	0.02197^{4}	0.02825^{8}	0.02487^{7}	0.02093^{3}	0.02293^{5}	0.03501^{9}	0.02344^{6}	0.01355^{2}	0.00993^{1}
		$\hat{b}$	0.03520^{5}	0.04126^{8}	0.03659^{7}	0.02753^{3}	0.03251^{4}	0.05276^{9}	0.03611^{6}	0.01662^{2}	0.01353^{1}
	MRE	$\hat{a}$	0.16271^{2}	0.18710^{8}	0.17657^{7}	0.16850^{4}	0.17234^{6}	0.20166^{9}	0.17191^{5}	0.16632^{3}	0.14238^{1}
		$\hat{b}$	0.15534^{4}	0.17028^{8}	0.16106^{7}	0.14939^{3}	0.15647^{5}	0.18728^{9}	0.16054^{6}	0.14324^{2}	0.12924^{1}
	$\sum$ Ranks		21^{4}	48^{8}	42^{7}	20^{3}	31^{5}	54^{9}	34^{6}	14^{2}	6^{1}
100	AB	$\hat{a}$	0.07965^{2}	$0.09430^{8.5}$	0.08512^{6}	0.08302^{5}	0.08844^{7}	$0.09430^{8.}$	0.08287^{4}	0.08197^{3}	0.06977^{1}
		$\hat{b}$	0.09519^{4}	0.10884^{8}	0.09945^{6}	0.09499^{3}	0.10269^{7}	0.11137^{9}	0.09709^{5}	0.08626^{2}	0.08045^{1}
	MSE	$\hat{a}$	0.01037^{3}	0.01422^{8}	0.01175^{6}	0.01046^{4}	0.01244^{7}	0.01457^{9}	0.01108^{5}	0.00672^{2}	0.00487^{1}
		$\hat{b}$	0.01495^{4}	0.01942^{8}	0.01657^{6}	0.01385^{3}	0.01713^{7}	0.02068^{9}	0.01545^{5}	0.00744^{2}	0.00647^{1}
	MRE	$\hat{a}$	0.11379^{2}	$0.13472^{8.5}$	0.1216^{6}	0.11860^{5}	0.12635^{7}	$0.13472^{8.}$	0.11838^{4}	0.11710^{3}	0.09967^{1}
		$\hat{b}$	0.10576^{4}	0.12093^{8}	0.11050^{6}	0.10554^{3}	0.11410^{7}	0.12374^{9}	0.10787^{5}	0.09584^{2}	0.08939^{1}
	$\sum$ Ranks		19^{3}	49^{8}	36^{6}	23^{4}	42^{7}	53^{9}	28^{5}	14^{2}	6^{1}
250	AB	$\hat{a}$	0.04984^{2}	0.05890^{8}	0.05380^{6}	0.05108^{4}	0.05546^{7}	0.05974^{9}	0.05176^{5}	0.05050^{3}	0.04442^{1}
		$\hat{b}$	0.05931^{3}	0.06813^{8}	0.06260^{6}	0.05956^{4}	0.06388^{7}	0.07036^{9}	0.06079^{5}	0.05493^{2}	0.05213^{1}
	MSE	$\hat{a}$	0.00400^{3}	0.00541^{8}	0.00456^{6}	0.00405^{4}	0.00488^{7}	0.00572^{9}	0.00425^{5}	0.00255^{2}	0.00197^{1}
		$\hat{b}$	0.00567^{4}	0.00740^{8}	0.00636^{6}	0.00546^{3}	0.00649^{7}	0.00801^{9}	0.00595^{5}	0.00302^{2}	0.00272^{1}
	MRE	$\hat{a}$	0.07120^{2}	0.08414^{8}	0.07685^{6}	0.07297^{4}	0.07923^{7}	0.08534^{9}	0.07394^{5}	0.07215^{3}	0.06346^{1}
		$\hat{b}$	0.06590^{3}	0.07570^{8}	0.06955^{6}	0.06618^{4}	0.07098^{7}	0.07818^{9}	0.06754^{5}	0.06103^{2}	0.05793^{1}
	$\sum$ Ranks		17^{3}	48^{8}	36^{6}	23^{4}	42^{7}	54^{9}	30^{5}	14^{2}	6^{1}

Table 14. Simulation results for the nine estimation methods for $a = 0.8$ and $b = 1.5$.

n	Est.	Par.	MLEs	LSEs	WLSEs	MPSEs	PCEs	CVMEs	ADEs	RTADEs	MMEs
20	AB	$\hat{a}$	0.19300^{5}	0.21391^{8}	0.20535^{7}	0.18749^{4}	0.19687^{6}	0.23955^{9}	0.18703^{3}	0.17909^{2}	0.16660^{1}
		$\hat{b}$	0.49531^{6}	0.52103^{8}	0.49822^{7}	0.40550^{3}	0.42100^{4}	0.67677^{9}	0.46378^{5}	0.37128^{2}	0.36738^{1}
	MSE	$\hat{a}$	0.06687^{6}	0.08045^{8}	0.07291^{7}	0.05296^{3}	0.06042^{5}	0.11243^{9}	0.05986^{4}	0.03207^{2}	0.02776^{1}
		$\hat{b}$	0.56002^{6}	0.73417^{8}	0.61027^{7}	0.30618^{3}	0.34277^{4}	5.03792^{9}	0.45580^{5}	0.13785^{2}	0.13497^{1}
	MRE	$\hat{a}$	0.24125^{5}	0.26738^{8}	0.25669^{7}	0.23436^{4}	0.24609^{6}	0.29943^{9}	0.23378^{3}	0.22386^{2}	0.20825^{1}
		$\hat{b}$	0.33021^{6}	0.34735^{8}	0.33214^{7}	0.27034^{3}	0.28067^{4}	0.45118^{9}	0.30918^{5}	0.24752^{2}	0.24492^{1}
	$\sum$ Ranks		34^{6}	48^{8}	42^{7}	20^{3}	29^{5}	54^{9}	25^{4}	12^{2}	6^{1}
50	AB	$\hat{a}$	0.11389^{3}	0.13315^{8}	0.12222^{7}	0.11838^{5}	0.12162^{6}	0.13795^{9}	0.11695^{4}	0.10910^{2}	0.10089^{1}
		$\hat{b}$	0.26745^{5}	0.30306^{8}	0.28041^{7}	0.25673^{3}	0.26012^{4}	0.33069^{9}	0.27223^{6}	0.23259^{2}	0.22743^{1}
	MSE	$\hat{a}$	0.02182^{4}	0.02877^{8}	0.02428^{7}	0.02111^{3}	0.02286^{6}	0.03205^{9}	0.02232^{5}	0.01190^{2}	0.01018^{1}
		$\hat{b}$	0.13333^{6}	0.17731^{8}	0.14059^{7}	0.10172^{3}	0.11152^{4}	0.20811^{9}	0.13139^{5}	0.05410^{2}	0.05173^{1}
	MRE	$\hat{a}$	0.14237^{3}	0.16644^{8}	0.15277^{7}	0.14798^{5}	0.15202^{6}	0.17243^{9}	0.14619^{4}	0.13638^{2}	0.12611^{1}
		$\hat{b}$	0.17830^{5}	0.20204^{8}	0.18694^{7}	0.17115^{3}	0.17341^{4}	0.22046^{9}	0.18149^{6}	0.15506^{2}	0.15162^{1}
	$\sum$ Ranks		26^{4}	48^{8}	42^{7}	22^{3}	$30^{5.5}$	54^{9}	$30^{5.5}$	12^{2}	6^{1}
100	AB	$\hat{a}$	0.07810^{2}	0.09244^{8}	0.08280^{6}	0.08043^{3}	0.08555^{7}	0.09280^{9}	0.08151^{5}	0.08059^{4}	0.07222^{1}
		$\hat{b}$	0.17727^{4}	0.20778^{8}	0.18965^{7}	0.17391^{3}	0.18648^{6}	0.21195^{9}	0.18487^{5}	0.16771^{2}	0.15790^{1}
	MSE	$\hat{a}$	$0.00993^{3.}$	0.01375^{8}	0.01103^{6}	$0.00993^{3.}$	0.01160^{7}	0.01403^{9}	0.01074^{5}	0.00649^{2}	0.00522^{1}
		$\hat{b}$	0.05390^{4}	0.07385^{8}	0.06027^{7}	0.04658^{3}	0.05553^{5}	0.07734^{9}	0.05732^{6}	0.02813^{2}	0.02493^{1}
	MRE	$\hat{a}$	0.09762^{2}	0.11555^{8}	0.10349^{6}	0.10054^{3}	0.10694^{7}	0.11600^{9}	0.10189^{5}	0.10074^{4}	0.09027^{1}
		$\hat{b}$	0.11818^{4}	0.13852^{8}	0.12643^{7}	0.11594^{3}	0.12432^{6}	0.14130^{9}	0.12325^{5}	0.11181^{2}	0.10527^{1}
	$\sum$ Ranks		19.5^{4}	48^{8}	39^{7}	18.5^{3}	38^{6}	54^{9}	31^{5}	16^{2}	6^{1}
250	AB	$\hat{a}$	0.04908^{3}	0.05828^{8}	0.05207^{6}	0.04963^{4}	0.05417^{7}	0.05868^{9}	0.05064^{5}	0.04902^{2}	0.04383^{1}
		$\hat{b}$	0.11023^{4}	0.12940^{8}	0.11614^{6}	0.10783^{3}	0.11759^{7}	0.13000^{9}	0.11432^{5}	0.10208^{2}	0.09742^{1}
	MSE	$\hat{a}$	0.00383^{4}	0.00527^{8}	0.00431^{6}	0.00382^{3}	0.00457^{7}	0.00550^{9}	0.00411^{5}	0.00240^{2}	0.00192^{1}
		$\hat{b}$	0.01952^{4}	0.02681^{8}	0.02200^{7}	0.01837^{3}	0.02184^{6}	0.02771^{9}	0.02106^{5}	0.01042^{2}	0.00949^{1}
	MRE	$\hat{a}$	0.06134^{3}	0.07284^{8}	0.06509^{6}	0.06204^{4}	0.06771^{7}	0.07335^{9}	0.06330^{5}	0.06128^{2}	0.05479^{1}
		$\hat{b}$	0.07348^{4}	0.08627^{8}	0.07742^{6}	0.07189^{3}	0.07839^{7}	0.08667^{9}	0.07621^{5}	0.06806^{2}	0.06495^{1}
	$\sum$ Ranks		22^{4}	48^{8}	37^{6}	20^{3}	41^{7}	54^{9}	30^{5}	12^{2}	6^{1}

Table 15. Partial and overall ranks of all estimation methods of the FExKw distribution for different values of a and b.

Est. Par.	n	MLEs	LSEs	WLSEs	MPSEs	PCEs	CVMEs	ADEs	RTADEs	MMEs
$a = 0.5, b = 0.5$	20	6	7	5	3	4	8.5	8.5	2	1
	50	4	7	5	2.5	6	8.5	8.5	2.5	1
	100	4	7	5	2	6	8.5	8.5	3	1
	250	3	6	5	2	7	9	8	4	1
$a = 0.2, b = 0.5$	20	5	6	4	2	7	8.5	8.5	3	1
	50	4	6	5	1	8.5	8.5	7	2.5	2.5
	100	2	6	5	1	9	7.5	7.5	3.5	3.5
	250	2	6	5	1	9	8	7	4	3
$a = 1.2, b = 3.5$	20	5	7	6	3	4	9	8	1.5	1.5
	50	4	8	6	3	5	9	7	2	1
	100	4	7	6	3	5	8.5	8.5	2	1
	250	3.5	7.5	6	3.5	5	9	7.5	2	1
$a = 1.7, b = 2.5$	20	5	7	6	4	3	9	8	2	1
	50	4.5	7	6	4.5	2.5	9	8	2.5	1
	100	5	7	6	4	3	9	8	2	1
	250	4.5	9	6	4.5	3	7	8	2	1
$a = 2.3, b = 2$	20	5	7	6	4	3	9	8	2	1
	50	4.5	7	6	4.5	3	9	8	2	1
	100	5	7	6	4	3	8.5	8.5	2	1
	250	3	9	6	4.5	4.5	8	7	2	1
$a = 1.3, b = 0.5$	20	4	7	5	3	6	8.5	8.5	2	1
	50	4	6	5	2	7	8.5	8.5	3	1
	100	3.5	6	5	2	7	8.5	8.5	3.5	1
	250	3	6	5	2	8	9	7	4	1
$a = 2.5, b = 2.5$	20	5	7.5	6	3.5	3.5	9	7.5	2	1
	50	5	7	6	4	3	9	8	2	1
	100	4	7	6	5	3	9	8	2	1
	250	5	8	6	3.5	3.5	9	7	2	1
$a = 3.5, b = 0.7$	20	6	8	5	3	7	9	4	2	1
	50	4.5	7	6	3	8	9	4.5	2	1
	100	4	7	6	2	9	8	5	3	1
	250	4	7	6	2	9	8	5	3	1
$a = 0.4, b = 1.25$	20	6	8	5	2	7	9	4	1	3
	50	2.5	7	6	2.5	8.5	8.5	5	1	4
	100	3	7	6	2	9	8	5	1	4
	250	2	8	6	3	9	7	5	1	4

Continued on next page

Est. Par.	n	MLEs	LSEs	WLSEs	MPSEs	PCEs	CVMEs	ADEs	RTADEs	MMEs
$a = 0.7, b = 0.9$	20	6	8	7	3	4	9	5	2	1
	50	4	8	7	3	5	9	6	2	1
	100	3	8	6	4	7	9	5	2	1
	250	3	8	6	4	7	9	5	2	1
$a = 0.8, b = 1.5$	20	6	8	7	3	5	9	4	2	1
	50	4	8	7	3	5.5	9	5.5	2	1
	100	4	8	7	3	6	9	5	2	1
	250	4	8	6	3	7	9	5	2	1
$\sum$ Ranks		182.5	318	254	131.5	254.5	380	299	99	61.5
Overall Rank		4	8	5	3	6	9	7	2	1

8. Real data analysis in various applied fields

This section demonstrates the practical value and flexibility of the proposed FExKw distribution through applications to real datasets. To do this, the model is fitted to four datasets drawn from different applied settings and then compared with the baseline distribution and several alternative models. These comparisons are used to assess how well the proposed distribution can capture bounded real-world data and to show that it offers a flexible and competitive fit.

The datasets considered in this section were chosen to reflect both practical importance and statistical variation. They were taken from different fields, including environmental, industrial, and medical research, where the analysis of non-negative continuous data is frequently required. In addition, the datasets display a range of distributional features, such as varying degrees of skewness, differences in their tail behavior, and distinct hazard rate shapes. This variety provides a useful basis for examining the adaptability and performance of the proposed FExKw model relative to the baseline and other competing distributions. Some of these datasets have also been used in earlier studies, which makes the comparisons more meaningful and strengthens the reproducibility of the findings.

The first dataset comprises 30 observations of daily snowfall amounts recorded in inches of water, derived from experimental units that were not subjected to seeding. The experiment took place near Climax, Colorado [37].

The data are 0.010, 0.030, 0.015, 0.020, 0.100, 0.045, 0.100, 0.190, 0.125, 0.390, 0.070, 0.110, 0.010, 0.220, 0.055, 0.080, 0.125, 0.005, 0.035, 0.060, 0.085, 0.010, 0.020, 0.065, 0.260, 0.015, 0.030, 0.025, 0.495, and 0.085.

The second dataset, originally analyzed by Dumonceaux and Antle [38], records the annual maximum flood levels of the Susquehanna River at Harrisburg, Pennsylvania, over a 20-year period. The measurements, expressed in millions of cubic feet per second, provide insights into the river's peak water flow each year. The recorded flood levels are as follows: 0.654, 0.613, 0.315, 0.449, 0.297, 0.402, 0.379, 0.423, 0.379, 0.324, 0.269, 0.740, 0.418, 0.412, 0.494, 0.416, 0.338, 0.392, 0.265, and 0.484.

The third dataset is sourced from Elgarhy et al. [39] and focuses on the strength measurements of 1.5-cm glass fibers. These measurements were originally collected by researchers at the UK National Physical Laboratory. The data include the following values: 0.13, 0.17, 0.12, 0.14, 0.16, 0.15, 0.20,

0.13, 0.15, 0.11, 0.20, 0.12, 0.36, 0.15, 0.38, 0.12, 0.16, 0.21, 0.16, 0.23, 0.33, 0.12, 0.32, 0.10, 0.33, 0.26, and 0.20.

The fourth dataset consists of the COVID-19 death rate values recorded in Spain between 3 March and 7 May 2020. It includes 60 observations, namely 0.5714, 0.2105, 0.2311, 0.48, 0.3625, 0.3922, 0.3414, 0.4288, 0.3939, 0.4076, 0.4079, 0.4408, 0.4046, 0.3836, 0.3545, 0.3275, 0.3162, 0.315, 0.3053, 0.293, 0.279, 0.2685, 0.2492, 0.2481,0.2453, 0.2355, 0.2285, 0.2241, 0.2193, 0.2162, 0.2153, 0.2129, 0.2037, 0.3127, 0.2066, 0.25, 0.2087, 0.2038, 0.2029, 0.2023, 0.1993, 0.1962, 0.1711, 0.1678, 0.1646, 0.1629, 0.1613, 0.1544, 0.151, 0.1484, 0.1465, 0.1453, 0.142, 0.1396, 0.1372, 0.333, 0.3711, 0.5, 0.2588, and 0.4839.

To estimate the model parameters, we use the ML technique, and the computations are carried out using R statistical software. The standard errors (SEs) reported in Tables 16–19 for the ML estimates are computed from the observed information matrix, defined as the negative Hessian of the log-likelihood function evaluated at the ML technique. In our R implementation, the Hessian matrix is computed numerically using finite-difference approximations via the optim function with the option hessian=TRUE. The variance covariance matrix is then obtained by inverting the observed information matrix, and the SEs are taken as the square roots of its diagonal elements. This approach is standard in likelihood-based inference when closed-form expressions for the Fisher information are not tractable. The convergence of the optimization algorithm was verified for all fitted models. We evaluate how well the FExKw model fits the data by comparing its performance against other established Kw models, including the Kw [40], transmuted-Kumaraswamy (TKw) [41], 2-parameter new flexible Kumaraswamy (NFKw) [42], log-Kumaraswamy (logKw) [43], and beta distributions (BE) [44].

Tables 16–19 present the ML estimates for each fitted model, with the corresponding SEs shown in parentheses, for the four datasets. To compare the competing distributions with the proposed FExKw model, we rely on a set of information criteria (ICs), including the negative log-likelihood ($-\hat{\ell}$), Bayesian IC (BIC), Akaike IC (AIC), Hannan–Quinn IC (HQIC), corrected AIC (CAIC), alongside goodness-of-fit measures including the Cramér–von Mises (W^*), Anderson–Darling (A^*), and Kolmogorov–Smirnov (KS) statistics with the KS p-values. The resulting fit measures are summarized in Tables 20–23. In all cases, the FExKw distribution yields the most favorable pattern, showing the lowest ICs and discrepancy values and the highest p-values among the fitted models, which supports its overall superiority in capturing the observed data.

Table 16. The ML estimates and SEs of the competing distributions for the first dataset.

Distribution	$\hat{a}$	$\hat{b}$	$\hat{\lambda}$
FExKw	0.5867 (0.1020)	3.9659 (1.2760)	-
Kw	0.8614 (0.1375)	6.8358 (2.3235)	-
TKw	0.9453 (0.1478)	5.8188 (2.6541)	0.6140 (0.3984)
NFKw	0.5535 (0.0980)	4.4292 (1.3456)	-
logKw	0.9437 (0.1480)	9.2229 (3.3988)	-
BE	0.8575 (0.1924)	7.8057 (2.2431)	

Table 17. The ML estimates and SEs of the competing distributions for the second dataset.

Distribution	$\hat{a}$	$\hat{b}$	$\hat{\lambda}$
FExKw	2.5160 (0.4787)	7.2891 (3.2250)	-
Kw	3.3638 (0.6033)	11.7932 (5.3615)	-
TKw	3.7259 (0.6490)	10.9619 (6.0357)	0.6142 (0.3751)
NFKw	2.3461 (0.4557)	7.7211 (3.2130)	-
logKw	4.5534 (0.7543)	90.1990 (63.9193)	-
BE	6.7594 (2.0953)	9.1140 (2.8525)	

Table 18. The ML estimates and SEs of the competing distributions for the third dataset.

Distribution	$\hat{a}$	$\hat{b}$	$\hat{\lambda}$
FExKw	1.8334 (0.2786)	19.0136 (9.1385)	-
Kw	2.4966 (0.3690)	43.7533 (23.4370)	-
TKw	2.6991 (0.3928)	45.4388 (27.6957)	0.4762 (0.3972)
NFKw	1.7275 (0.2664)	19.5109 (8.8035)	-
logKw	2.8196 (0.4104)	100.2657 (63.8433)	-
BE	5.0742 (1.3391)	21.1243 (5.7892)	

Table 19. The ML estimates and SEs of the competing distributions for the fourth dataset.

Distribution	$\hat{a}$	$\hat{b}$	$\hat{\lambda}$
FExKw	1.8881 (0.2049)	10.3367 (2.9408)	-
Kw	2.6898 (0.2775)	23.1373 (7.3543)	-
TKw	2.8987 (0.2948)	21.8132 (8.7972)	0.5136 (0.3730)
NFKw	1.7925 (0.1974)	11.1684 (2.9956)	-
logKw	3.2092 (0.3218)	72.9854 (29.9606)	-
BE	5.0126 (0.8879)	13.3359 (2.4374)	

The empirical results presented in Tables 20–23 provide practical insight into model selection. According to the considered applications, the FExKw model appears to be particularly useful when (i) the data exhibit nonmonotone hazard rate behavior that is not adequately captured by the baseline Kw model; (ii) goodness-of-fit measures such as AIC, BIC, and KS indicate that the baseline model is too restrictive for the observed data structure; and (iii) parsimony is desirable, especially in small to moderate sample settings. Across the four real data applications considered in this study, the FExKw model was highly competitive and, in several cases, provided a better fit than the baseline and competing alternatives, supporting its practical value as a parsimonious yet flexible extension of the Kw distribution.

Table 20. Results of the goodness-of-fit statistics for the first dataset.

Distribution	$-\hat{\ell}$	AIC	CAIC	BIC	HQIC	A^*	W^*	KS	p-value
FExKw	-41.0997	-78.1995	-77.7551	-75.3971	-77.3030	0.2661	0.0338	0.0797	0.99105
Kw	-39.7976	-75.5952	-75.1507	-72.7928	-74.6987	0.4769	0.0629	0.1207	0.77419
TKw	-40.3972	-74.7944	-73.8713	-70.5908	-73.4496	0.3771	0.0483	0.0998	0.92598
NFKw	-40.8395	-77.6791	-77.2347	-74.8767	-76.7826	0.3074	0.0388	0.0870	0.97701
logKw	-40.3208	-76.6416	-76.1971	-73.8392	-75.7451	0.3680	0.0470	0.1027	0.90915
BE	-39.5608	-75.1217	-74.6773	-72.3193	-74.2252	0.5210	0.0695	0.1287	0.7023

Table 21. Results of the goodness-of-fit statistics for the second dataset.

Distribution	$-\hat{\ell}$	AIC	CAIC	BIC	HQIC	A^*	W^*	KS	p-value
FExKw	-14.6420	-25.2840	-24.5781	-23.2925	-24.8953	0.6120	0.0996	0.1706	0.6053
Kw	-12.8685	-21.7371	-21.0312	-19.7456	-21.3483	0.9726	0.1659	0.2109	0.3354
TKw	-13.5235	-21.0471	-19.5471	-18.0599	-20.4640	0.8411	0.1410	0.1930	0.4451
NFKw	-14.2408	-24.4817	-23.7758	-22.4902	-24.0929	0.6968	0.1147	0.1798	0.5374
logKw	-13.8563	-23.7125	-23.0067	-21.7211	-23.3238	0.1238	0.7484	0.1911	0.4582
BE	-14.0651	-24.1302	-23.4243	-22.1387	-23.7415	0.7526	0.1258	0.1988	0.4076

Table 22. Results of the goodness-of-fit statistics for the third dataset.

Distribution	$-\hat{\ell}$	AIC	CAIC	BIC	HQIC	A*	W*	KS	p-value
FExKw	-32.4428	-60.8856	-60.3856	-58.2940	-60.1150	1.0661	0.1681	0.1687	0.4255
Kw	-30.6731	-57.3462	-56.8462	-54.7545	-56.5755	1.4400	0.2377	0.1911	0.2771
TKw	-31.1657	-56.3313	-55.2879	-52.4438	-55.1754	1.3388	0.2184	0.1833	0.3243
NFKw	-32.0281	-60.0562	-59.5562	-57.4646	-59.2856	1.1519	0.1835	0.1755	0.3763
logKw	-31.1049	-58.2099	-57.7099	-55.6182	-57.4392	1.3429	0.2190	0.1877	0.2971
BE	-32.2712	-60.5425	-60.0425	-57.9508	-59.7719	1.1571	0.1854	0.1927	0.2683

Table 23. Results of the goodness-of-fit statistics for the fourth dataset.

Distribution	$-\hat{\ell}$	AIC	CAIC	BIC	HQIC	A*	W*	KS	p-value
FExKw	-53.6395	-103.2791	-103.0686	-99.0904	-101.6407	0.9450	0.1606	0.1033	0.5102
Kw	-51.2282	-98.4565	-98.2460	-94.2678	-96.8181	1.3037	0.2253	0.1364	0.1952
TKw	-51.9900	-97.9800	-97.5515	-91.6970	-95.5224	1.1953	0.2066	0.1268	0.2660
NFKw	-53.1717	-102.3434	-102.1329	-98.1547	-100.705	1.0245	0.1756	0.1133	0.3948
logKw	-52.2753	-100.5507	-100.3401	-96.3619	-98.9122	1.1553	0.1994	0.1274	0.2607
BE	-53.6171	-103.2344	-103.0239	-99.0456	-101.596	0.9895	0.1697	0.1238	0.2914

Figures 8–11 display the fitted density along with the empirical and fitted CDF, SF, and probability–probability (PP) plots for the four datasets. Overall, the FExKw model provides a close fit to the data, as evidenced by the agreement between the fitted and empirical CDF/SF curves and the near-linear PP plots, with only minor deviations in the tails. These results suggest that the FExKw distribution is a suitable model for the datasets considered and can accommodate a range of skewness patterns.

Although the simulation study in Section 7 indicates that alternative estimators such as MMEs and RTADEs may exhibit superior finite-sample performance for parameter estimation under certain configurations, we use ML technique for the real data applications in this section for several reasons. First, ML technique is the standard method used in the literature for fitting and comparing the competing distributions considered here (Kw, TKw, NFKw, logKw, BE), ensuring a consistent and fair benchmark. Second, the information criteria (AIC, BIC, CAIC, HQIC) and goodness-of-fit statistics used for model comparison are theoretically grounded in the likelihood framework, making MLE the natural choice for these assessments. Third, preliminary analyses showed that the parameter estimates and model rankings were stable across different estimation methods for these datasets, supporting the robustness of our conclusions.

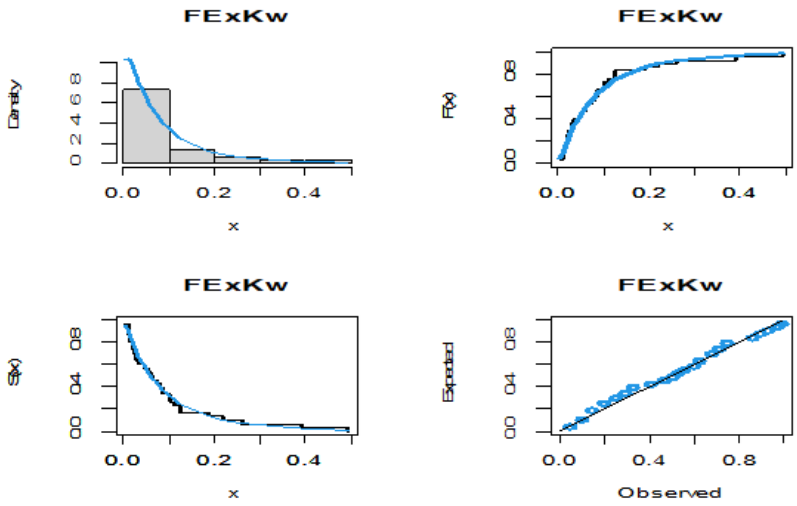


Figure 8. Plots of the fitted FExKw model functions for the first dataset.

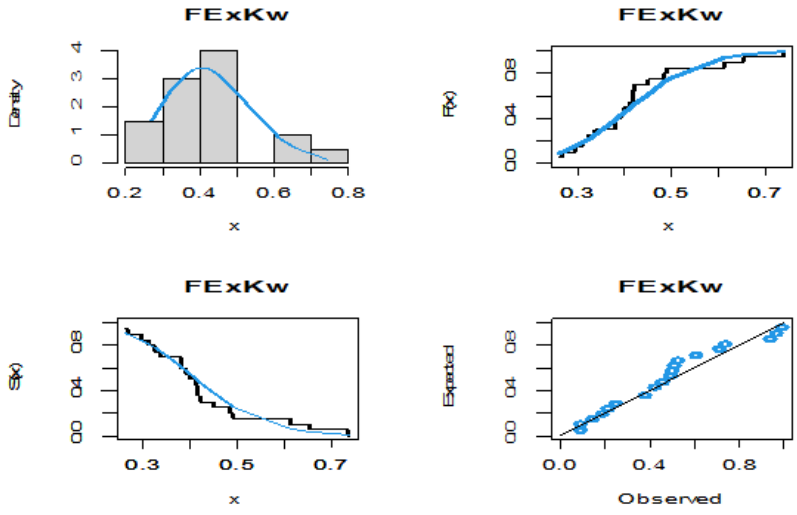


Figure 9. Plots of the fitted FExKw model functions for the second dataset.

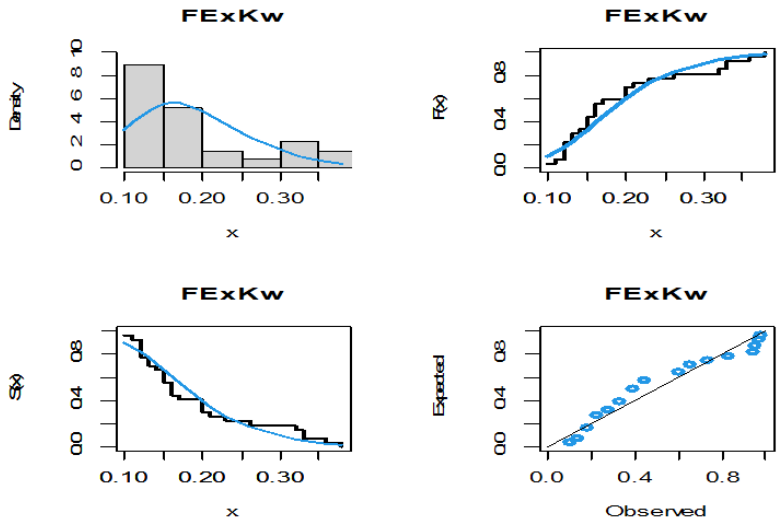


Figure 10. Plots of the fitted FExKw model functions for the third dataset.

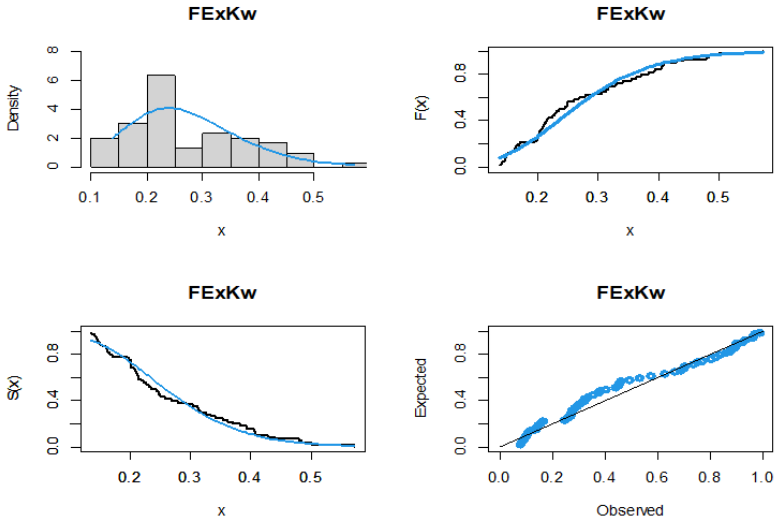


Figure 11. Plots of the fitted FExKw model functions for the fourth dataset.

9. Conclusions and future perspectives

In this paper, we introduced and studied the FEx-G family as a parsimonious transformation-based extension of baseline distributions. Several submodels of this family were found to exhibit a wide range of density and hazard rate behaviors under suitable parameter settings. A mixture representation of the FEx-G family in terms of the exponentiated-G family was also derived, and the main mathematical properties of the proposed family were investigated. Particular attention was given to the FExKw submodel, for which the behavior of the failure rate and mean residual life functions was analyzed in detail. In addition, nine estimation methods were considered for estimating the parameters of the FExKw model. The simulation results showed that all estimators

performed reasonably well, with the MM method providing the best overall performance among the methods considered. The practical usefulness of the FExKw distribution was further illustrated by four real datasets, where the model was highly competitive and, in several cases, provided a better fit than the competing exponential-based models considered in this study.

Several directions for future research naturally arise from the present study. First, the detailed theoretical and inferential analysis can be extended to other submodels of the proposed FEx-G family that were introduced but not investigated in depth in this paper, such as the FEx-Weibull, FEx-exponential, FEx-gamma, and FEx-beta distributions. Future studies may focus on deriving and examining their main mathematical properties, including the behavior of the HRF and other related reliability characteristics. It would also be of interest to evaluate their inferential performance under different estimation methods and to investigate their practical usefulness through applications to real datasets from a variety of fields. Such extensions would provide a broader understanding of the flexibility, usefulness, and applicability of the proposed FEx-G framework.

Author contributions

Eman. M. Eldemery, Hisham M. Almongy and Khaled M. Mahfouz: Methodology, Formal analysis, Investigation, Resources, Writing-original draft preparation, Writing-review and editing; Mohammed M. El Genidy, Ibrahim Elbatal, Hassan M. Aljohani and Ahmed Z. Afify: Conceptualization, Software, Validation, Writing-original draft preparation, Writing-review and editing. All authors have read and approved the final version of the manuscript for publication.

Use of Generative AI tools declaration

The authors declare they have not used artificial intelligence (AI) tools in the creation of this article.

Funding

This work was supported and funded by the Deanship of Scientific Research at Imam Mohammad Ibn Saud Islamic University (IMSIU) (grant number IMSIU-DDRSP2602).

Conflict of interest

The authors declare no conflict of interest.

References

[1] G. M. Cordeiro, M. de Castro, A new family of generalized distributions, *J. Stat. Comput. Sim.*, **81** (2011), 883–898. https://doi.org/10.1080/00949650903530745

[2] H. M. Yousof, A. Z. Afify, M. Alizadeh, N. S. Butt, G. Hamedani, M. M. Ali, The transmuted exponentiated generalized-G family of distributions, *Pak. J. Stat. Oper. Res.*, **11** (2015), 441–464. https://doi.org/10.18187/pjsor.v11i4.1164

[3] M. Bourguignon, R. B. Silva, G. M. Cordeiro, The Weibull-G family of probability distributions, *J. Data Sci.*, **12** (2014), 53–68.

[4] A. W. Marshall, I. Olkin, A new method for adding a parameter to a family of distributions with applications to the exponential and Weibull families, *Biometrika*, **84** (1997), 641–652. https://doi.org/10.1093/biomet/84.3.641

[5] W. T. Shaw, I. R. C. Buckley, The alchemy of probability distributions: beyond Gram-Charlier expansions and a skew-kurtotic-normal distribution from a rank transmutation map, 2007, arXiv:0901.0434. https://doi.org/10.48550/arXiv.0901.0434

[6] A. Z. Afify, G. M. Cordeiro, H. M. Yousof, A. Alzaatreh, Z. M. Nofal, The Kumaraswamy transmuted-G family of distributions: properties and applications, *J. Data Sci.*, **14** (2016), 245–270. https://doi.org/10.6339/JDS.201604_14(2).0004

[7] G. M. Cordeiro, M. Alizadeh, G. Ozel, B. Hosseini, E. M. M. Ortega, E. Altun, The generalized odd log-logistic family of distributions: Properties, regression models and applications, *J. Stat. Comput. Sim*., **87** (2017), 908–932. https://doi.org/10.1080/00949655.2016.1238088

[8] A. Z. Afify, H. Al-Mofleh, H. M. Aljohani, G. M. Cordeiro, The Marshall-Olkin-Weibull-H family: estimation, simulations, and applications to COVID-19 data, *J. King Saud Univ. Sci*., **34** (2022), 102115. https://doi.org/10.1016/j.jksus.2022.102115

[9] N. Eugene, C. Lee, F. Famoye, Beta-normal distribution and its applications, *Commun. Stat.-Theor. M.*, **31** (2002), 497–512. https://doi.org/10.1081/STA-120003130

[10] M. S. Shama, F. El Ktaibi, J. N. Al Abbasi, C. Chesneau, A. Z. Afify, Complete study of an original power-exponential transformation approach for generalizing probability distributions, *Axioms*, **12** (2023), 67. https://doi.org/10.3390/axioms12010067

[11] Z. M. Nofal, A. Z. Afify, H. M. Yousof, H. G. M. Cordeiro, The generalized transmuted-G family of distributions, *Commun. Stat.-Theor. M.*, **46** (2017), 4119–4136. https://doi.org/10.1080/03610926.2015.1078478

[12] T. Iqbal, F. M. Alghamdi, A. S. Alghamdi, F. Jamal, A. Z. Afify, The flexible Lomax-G family with estimation methods and applications in hydrology and biomedicine, *Sci. Rep*., **15** (2025), 33321. https://doi.org/10.1038/s41598-025-18655-x

[13] J. N. Al Abbasi, I. Elbatal, A. Z. Afify, H. A. Mahran, A novel flexible exponential-G family: Properties, estimation, and applications in environmental and engineering sciences, *J. King Saud Univ. Sci*., **37** (2025), 8202025. https://doi.org/10.25259/JKSUS_820_2025

[14] A. Z. Afify, M. M. Helmi, H. M. Aljohani, S. M. A. Alsheikh, H. A. Mahran, Modeling lifetime and count data using a unified flexible family: Its discrete counterpart, properties, and inference, *PLoS ONE*, **20** (2025), e0319091. https://doi.org/10.1371/journal.pone.0319091

[15] P. Kavya, M. Manoharan, Some parsimonious models for lifetimes and applications, *J. Stat. Comput. Sim*., **91** (2021), 3693–3708. https://doi.org/10.1080/00949655.2021.1946064

[16] O. H. M. Hassan, I. Elbatal, A. H. Al-Nefaie, M. Elgarhy, On the Kavya-Manoharan-Burr X model: Estimations under ranked set sampling and applications, *J. Risk Financial Manag.*, **16** (2023), 19. https://doi.org/10.3390/jrfm16010019

[17] N. Alotaibi, A. F. Hashem, I. Elbatal, S. A. Alyami, A. S. Al-Moisheer, M. Elgarhy, Inference for a Kavya-Manoharan inverse length biased exponential distribution under progressive-stress model based on progressive type-II censoring, *Entropy*, **24** (2022), 1033. https://doi.org/10.3390/e24081033

[18] A. H. Al-Nefaie, Applications to bio-medical data and statistical inference for a Kavya-Manoharan log-logistic model, *J. Radiat. Res. Appl. Sci*., **16** (2023), 100523. https://doi.org/10.1016/j.jrras.2023.100523

[19] N. Alotaibi, I. Elbatal, M. Shrahili, A. S. Al-Moisheer, M. Elgarhy, E. M. Almetwally, Statistical inference for the Kavya-Manoharan Kumaraswamy model under ranked set sampling with applications, *Symmetry*, **15** (2023), 587. https://doi.org/10.3390/sym15030587

[20] E. A. Eldessouky, O. H. Hassan, M. Elgarhy, E. A. A. Hassan, I. Elbatal, E. M. Almetwally, A new extension of the Kumaraswamy exponential model with modeling of food chain data, *Axioms*, **12** (2023), 379. https://doi.org/10.3390/axioms12040379

[21] F. H. Riad, A. Radwan, E. M. Almetwally, M. Elgarhy, A new heavy tailed distribution with actuarial measures, *J. Radiat. Res. Appl. Sci*., **16** (2023), 100562. https://doi.org/10.1016/j.jrras.2023.100562

[22] R. C. Gupta, P. L. Gupta, R. D. Gupta, Modeling failure time data by Lehman alternatives, *Commun. Stat.-Theor. M.*, **27** (1999), 887–904. https://doi.org/10.1080/03610929808832134

[23] D. C. T. Granzotto, F. Louzada, N. Balakrishnan, Cubic rank transmuted distributions: inferential issues and applications, *J. Stat. Comput. Sim*., **87** (2016), 2760–2778. https://doi.org/10.1080/00949655.2017.1344239

[24] G. M. Cordeiro, E. M. M. Ortega, D. C. C. de Cunha, The exponentiated generalized class of distributions, *J. Data Sci*., **11** (2013), 1–27. https://doi.org/10.6339/JDS.2013.11(1).1086

[25] M. Bouhadjar, A. Djebar, H. Zeghdoudi, On Bouhadjar distribution: mathematical properties, simulation and applications, *Boletim da Sociedade Paranaense de Matemática*, **43** (2025), 1–12. https://doi.org/10.5269/bspm.77897

[26] N. Saaidia, R. Pakyari, H. Zeghdoudi, The Q-Lindley distribution: goodness-of-fit tests, modeling, inference, and applications, *J. Stat. Theory Appl*., **25** (2026), 6. https://doi.org/10.1007/s44199-025-00148-5

[27] H. Messaadia, H. Zeghdoudi, On Xbeta distribution: properties, estimation and application, *Boletim da Sociedade Paranaense de Matemática*, **43** (2025), 1–13. https://doi.org/10.5269/bspm.78451

[28] M. M. El Genidy, E. A. Hebeshy, B. E. El Desouky, R. S. Gomaa, An accurate method for estimating the parameters of the generalized extreme value distribution using its moments, *Alfarama Journal of Basic Applied Sciences*, **5** (2024), 190–207.

[29] Z. Afify, E. A. Elsherpieny, A. M. El-sheikh, G. M. Cordeiro, A generalized flexible family: theoretical properties, estimation, and risk analysis, *Benha J. Humanit. Sci.*, **5** (2026), 431–465.

[30] Alzaatreh, C. Lee, F. Famoye, A new method for generating families of continuous distributions, *Metron*, **71** (2013), 63–79. https://doi.org/10.1007/s40300-013-0007-y

[31] J. Mi, Bathtub failure rate and upside-down bathtub mean residual life, *IEEE T. Reliab*., **44** (1995), 388–391. https://doi.org/10.1109/24.406570

[32] R. C. H. Cheng, N. A. K. Amin, Maximum product-of-spacings estimation with applications to the lognormal distribution, *Math. Rep.*, **79** (1979), 1.

[33] R. C. H. Cheng, N. A. K. Amin, Estimating parameters in continuous univariate distributions with a shifted origin, *J. R. Stat. Soc. B*, **45** (1983), 394–403. https://doi.org/10.1111/j.25176161.1983.tb01268

[34] J. H. K. Kao, Computer methods for estimating Weibull parameters in reliability studies, *IRE Transactions on Reliability and Quality Control*, **13** (1958), 15–22. https://doi.org/10.1109/IRE-PGRQC.1958.5007164
[35] H. Cramér, On the composition of elementary errors, *Scand. Actuar. J.*, **1928** (1928), 13–74. https://doi.org/10.1080/03461238.1928.10416862
[36] R. E. Von Mises, *Wahrscheinlichkeit statistik und wahrheit*, Berlin: Springer, 1928. https://doi.org/10.1007/978-3-662-36230-3
[37] P. W. Mielke, L. O. Grant, C. F. Chappell, An independent replication of the Climax wintertime orographic cloud seeding experiment, *J. Appl. Meteorol. Clim.*, **10** (1971), 1198–1212.
[38] R. Dumonceaux, C. E. Antle, Discrimination between the lognormal and the Weibull distributions, *Technometrics*, **15** (1973), 923–926. https://doi.org/10.2307/1267401
[39] M. Elgarhy, M. A. Haq, Q. U. Ain, Exponentiated generalized Kumaraswamy distribution with applications, *Ann. Data Sci.*, **5** (2018), 273–292. https://doi.org/10.1007/s40745-017-0128-x
[40] P. Kumaraswamy, A generalized probability density function for double-bounded random processes, *J. Hydrol.*, **46** (1980), 79–88. https://doi.org/10.1016/0022-1694(80)90036-0
[41] M. S. Khan, R. King, L. I. Hudson, Transmuted Kumaraswamy distribution, *Statistics in Transition*, **17** (2016), 183–210. https://doi.org/10.59170/stattrans-2016-009
[42] M. H. Tahir, M. A. Hussain, G. M. Cordeiro, A new flexible generalized family for constructing many families of distributions, *J. Appl. Stat.*, **49** (2022), 1615–1635. https://doi.org/10.1080/02664763.2021.1874891
[43] I. Ishaq, A. A. Suleiman, H. Daud, N. S. S. Singh, M. Othman, R. Sokkalingam, et al., Log-Kumaraswamy distribution: its features and applications, *Front. Appl. Math. Stat.*, **9** (2023), 1–13. https://doi.org/10.3389/fams.2023.1258961
[44] N. L. Johnson, S. Kotz, N. Balakrishnan, *Continuous univariate distributions*, Hoboken: John Wiley & Sons, 1994.



AIMS Press

© 2026 the Author(s), licensee AIMS Press. This is an open access article distributed under the terms of the Creative Commons Attribution License (https://creativecommons.org/licenses/by/4.0)